Lehigh University
Lehigh Preserve

Theses and Dissertations

1990

A compliant insertion model for assembly systems with tolerance and precision

Michael F. Laub
Lehigh University

Follow this and additional works at: https://preserve.lehigh.edu/etd

Part of the Mechanical Engineering Commons

A COMPLIANT INSERTION MODEL FOR ASSEMBLY SYSTEMS WITH TOLERANCE AND PRECISION

By

Michael F. Laub

A Thesis

Presented to the Graduate Committee

of Lehigh University

in Candidacy for the Degree of

Master of Science

in

Mechanical Engineering and Mechanics Department

Lehigh University

September 1989

This thesis is accepted and approved in partial fulfillment of the requirements for the degree of Master of Science.

Sept. 14, 1989

Professor in Charge
Noel D. Perreira

Chairman of Department
Fazil Erdogan

Acknowledgements

Table of Contents

v

List of Tables

List of Figures

Abstract

Robust automated component insertion systems which consistently perform successfully are a growing need in industry. Design for assembly techniques have addressed this problem area in a number of different ways. In the proposed method, part dimensioning, tolerances, and equipment precision are related to the ability of the equipment to successfully perform the desired assembly. The result being tools that ensure the compatibility of a product design with the automated manufacturing process being used to produce it's assemblies. The method is cast in terms of a dimensionless part size ratio and the probability of successful assembly. In this paper we present the results of an experiment that show when the size ratio is modified to include compliance, it can be used to accurately predict the ability to assemble parts in a less than certain environment.

1

CHAPTER 1

INTRODUCTION

The concept of design for assembly has been around for several years and there has been a great deal of research performed [1-12]. The essence of design for assembly is the integration of the product design with the development of the assembly process. The objectives are two fold: 1) the design of the product for ease of assembly and 2) interfacing the product development and the assembly process design to ensure the most effective use of resources [1]. Interaction between product engineering and manufacturing is encouraged and utilized to improve the quality of the end product [2]. The design and manufacturing responsibilities are integrated, simultaneous, and ideally under the coordination of one authority. The product design and the capability of the manufacturing method are compatible in an integrated system [3]. Independent of the degree of automation, (manual, semi-automatic, hard, or flexible manufacturing), product designs which can be manufactured in a bottom up layered fashion are preferred [1,4]. Assembly tasks are applied in the vertical plane and each component positively located with the next.

In any insertion operation alignment of the components is an important consideration. Active and passive strategies for adding compliance have been applied to the automated assembly process to improve the alignment and mating of components [4]. The use of spring loaded fixtures, grippers and Remote Center Compliance or RCC devices are common examples of the passive strategy. Adding chamfers or increasing the clearance between mating parts is also used in an attempt to compensate for misalignment. The affect of the chamfer or clearance is an increase in assembly compliance [5].

Active strategies require the assembly equipment to respond to feedback from sensory inputs. In many applications a force/torque sensor is used to promote effective error recovery routines. The force/torque information is utilized in determining the resulting path of the robot, or logic branching is used to generate a series of move-and-bump cycles. Great care must be taken when applying active control strategies to ensure that the process does not become unstable.

The ability to successfully insert components in the assembly process becomes more sensitive to system parameters as the speed and automation of the process increase. In this study we examine a particular set of these parameters; namely part tolerances, the dimension of the parts, and the equipment precision. We also determine how equipment and part compliance produce an increase in the effective clearance between mating parts.

Tolerancing can have both adverse and beneficial influences on part alignment. Larger clearances and tolerances are commonly used to minimize the affect of poor equipment precision. Tolerance stacking, when using several dimensions can make an assembly untenable [6]. Tolerancing techniques produce or reduce much of the variability inherent in industrially manufactured parts.

The method presented in this paper assumes the use of geometric tolerances. Geometric dimensioning and tolerancing have been developed to control form and define limits of acceptability along with providing a means of specifying the interaction of size and location tolerances. The system requires features to be dimensioned from datums, eliminating tolerancing stack-up [7]. When applied to mating parts, the method allows for greater feature variation than bilateral techniques while ensuring successful assembly. This can significantly decrease the cost of a product.

The scope of this paper is limited to the analysis of the circular peg in circular hole problem but can easily be extended to very complex geometric forms [8]. This geometry is chosen for its simplicity and commonality to many industrial products [4,5,6,9,10,11,12]. When inserting one part into another, forces and torques may occur on the components and fixturing as the components mate. A circular cross-section minimizes the number of variables involved. The study is also limited to a particular set of dynamic parameters, in an attempt to gain an understanding of the fundamental interactions between tolerances, dimensions, and precisions.

CHAPTER 2

RIGID SYSTEM THEORY

Introduction

When a peg is inserted into a hole there are a number of parameters which can affect the success of the mating process. These parameters cause the center lines of the hole and peg to deviate laterally and angularly from each other. The misalignment results from imprecision of the device inserting the peg or the fixture which contains the part with the hole or from tolerancing generated in either the peg or hole. Typically, parts are designed to afford a certain amount of clearance during mating. The clearance is required to overcome any errors accrued by the manufacturing equipment along with the dimensional errors associated with each component. When the variations of the components and the equipment do not meet a minimum level, a collision or jam will occur that reduces the productivity of the process.

The productivity of the assembly process can be expressed in terms of a Probability of Successful Assembly or PSA. The PSA gives the design engineer the ability to determine the required clearance and tolerance specification of the mating parts to ensure a specified level of productivity, when the positioning errors of the assembly equipment is known. The PSA can also be used to assist the manufacturing engineer in the selection of the required part processing equipment given the dimensional and tolerance specifications set by the designer and knowledge of the allowable insertion failure rate. The PSA thus becomes a tool in integrating process and product design.

Maximum Allowable Size Ratio

Several models have been developed which take into account the size ratio, part tolerancing and equipment precision factors for determining the PSA of an assembly process [6,8,9,10]. This is a fundamental break from typical design where clearance selection is based on experience or empirical methods. The analytical approach developed by Doydum [8] is used here. The primary design variable in this method is the non-dimensional size ratio, $SR = d_p/d_h$. d_h is the mean diameter of the hole, and d_p is the mean diameter of the peg as shown in Fig. 1. Data obtained from a
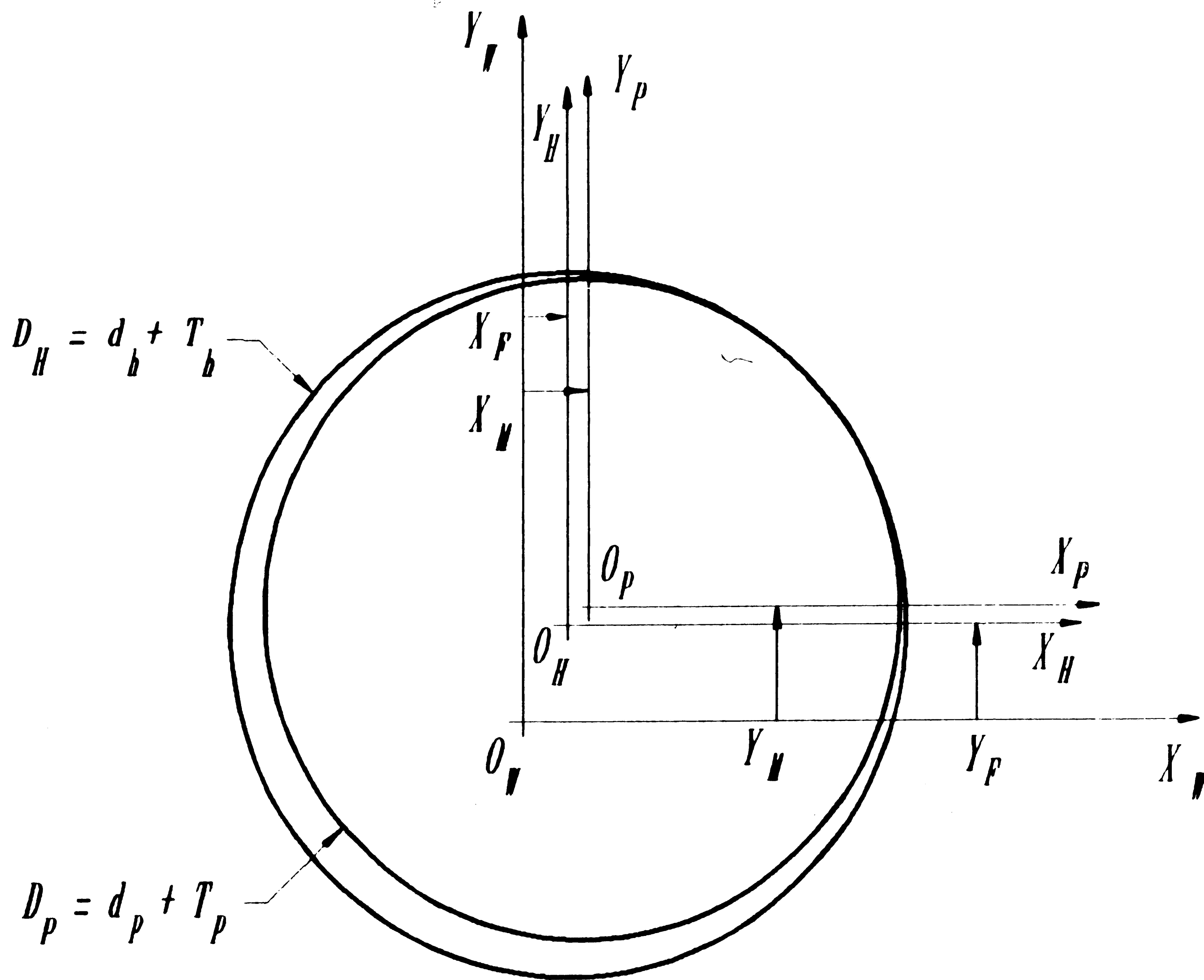
Figure 1. Theoretical Model Error Parameters

$D_H = d_h + T_h$

$D_p = d_p + T_p$

computer program based on his theory forms the initial core of information used to develop the modified or compliant insertion model found in this study.

The actual diameters of the peg and hole, D_P, D_H, are represented by probability distributions which are assumed normal: $N(d_p, \sigma_p)$ for the pin, and $N(d_h, \sigma_h)$ for the hole. The diameters for the peg and hole are separated into deterministic and stochastic components; $D_P = d_p + T_p$, where $T_p \sim N(0, \sigma_p)$ and $D_H = d_h + T_h$, where $T_h \sim N(0, \sigma_h)$. The repeatability demonstrated manipulator and fixture positioning errors are represented by M and F respectively. It is assumed that the fixture and manipulator positioning have been so calibrated as to eliminate or not be affected by accuracy errors. They are also assumed mutually independent. The X and Y components of each are taken to be independent; $M_x \sim N(0, \sigma_{Mx})$, $M_y \sim N(0, \sigma_{My})$ and $F_x \sim N(0, \sigma_{Fx})$, $F_y \sim N(0, \sigma_{Fy})$. The parameters: σ_P, σ_H, σ_{Mx}, σ_{My}, σ_{Fx}, σ_{Fy} are the standard deviations of the tolerances and repeatability associated with the pin, hole, manipulator, and fixture, respectively.

The random variable for the maximum allowable size ratio is defined as the largest acceptable ratio of actual peg diameter to mean hole diameter given the error conditions generated by T_h, T_p, F_x, F_y, M_x, M_y. The ratio is found using Fig. 1, resulting in:

$$SR = \frac{D_p}{d_h} = \frac{d_h + T_h - T_p - 2\,[(F_x - M_x)^2 + (F_y - M_y)^2]^{1/2}}{d_h} \tag{1}$$

Manipulator and fixture errors, M and F are shown as having magnitude in opposing directions. This produces the maximum error condition for the circular geometry in the two dimensional model.

Probability of Successful Assembly

The probability of successful insertion is determined by computing the area under the density function to the right of a given size ratio, sr. The probability density function for the maximum allowable size ratio is obtained by convolving the density functions of parameters it is dependent

6

upon.

The probability distribution for the difference of the pin and hole tolerances: $T_{hp} = T_h - T_p$, has a normal distribution $N(0, \sigma_{hp})$ defined in the interval $(-\infty, +\infty)$, to be,

$$f_{Thp}(x) = \frac{1}{\sigma_{hp}\sqrt{2\pi}}\, e^{-1/2(2x/\sigma_{hp})^2} \tag{2}$$

The normal distribution assumption for the repeatabilities has an effect on the positioning probability distributions for the manipulator and fixture. When two random variables with normal distributions are squared and added together, and then a square root is taken on the resulting sum a Rayleigh distribution is created [8].

$$f_{FM}(y) = \frac{y}{\sigma_{FM}^2}\, e^{-1/2(y/\sigma_{FM})^2} \tag{3}$$

These two functions are combined to form the joint probability density function of $E = T_{hp} - FM$:

$$f_E(z) = \frac{-\sigma_{FM}}{2(\sigma_{FM}^2 + \sigma_{hp}^2/4)^{3/2}}\, e^{\left[\frac{-z^2}{2(\sigma_{hp}^2/4 + \sigma_{FM}^2)}\right]}$$

$$\times\; \mathrm{erfc}\left[\frac{1}{\sqrt{2}\,\sigma_{hp}/4}\frac{\sigma_{FM}}{\sqrt{\sigma_{hp}^2/4 + \sigma_{FM}^2}}\right] z \;+\; \frac{\sigma_{hp}/2}{\sqrt{2\pi}\,(\sigma_{hp}^2/4 + \sigma_{FM}^2)}\, e^{\left[-2z^2/\sigma_{hp}\right]} \tag{4}$$

The probability density function for the maximum allowable size ratio is obtained after replacing z by z-1 and rescaling the tolerances and precision standard deviations by $2/d_h$. The area under the curve to the right of a given size ratio provides the probability of successful assembly for that size ratio.

7

$$PSA_{SR} = \int_{sr}^{\infty} f_{SR}(z) \; dz \qquad (5)$$

A Theoretical Example

Figure 2 shows a graph of the theoretical results for the PSA over size ratios ranging from .618 to .983. The tolerances of the peg and hole are both zero in the case where the same peg and hole are used in each attempt. Similarly for the fixture. In theoretical modelled case all variation is generated by the robot.

Regression analysis of the resulting theoretical data is employed in order to produce a simple analytical curve that could be used in later analysis. The Weibull relationship indicates that the PSA at a particular size ratio, SR is given by [13]:

$$PSA = e^{-(\alpha \times SR^{\beta})} \qquad (6)$$

The Weibull parameters α and β are obtained by first converting the Weibull function into a linear equation of the natural logarithms of the parameters:

$$\ln \ln (1/PSA) = \ln \alpha + \beta \ln SR \qquad (7)$$

The linear regression is performed and the resulting data is converted back to the exponential form as shown in Fig. 2. The standard error between the curve fit and the theoretical data is less than the error of the various numerical methods required to generate the theoretical data.

Experimental Apparatus

An experiment was performed to verify the appropriateness of the theoretical method. The

8

Theoretical and Regression Results
Size Ratio vs PSA

Program Input

$\sigma_{Manipulator} = .008$
$\sigma_{Fixture} = 0$
$T_P = 0$
$T_H = 0$

Regression Analysis Parameters

$$PSA = e^{-\alpha SR^{\beta}}$$

$\alpha = 5.337154$
$\beta = 8.080926$
$\sigma = .088310$

Size Ratio

PSA
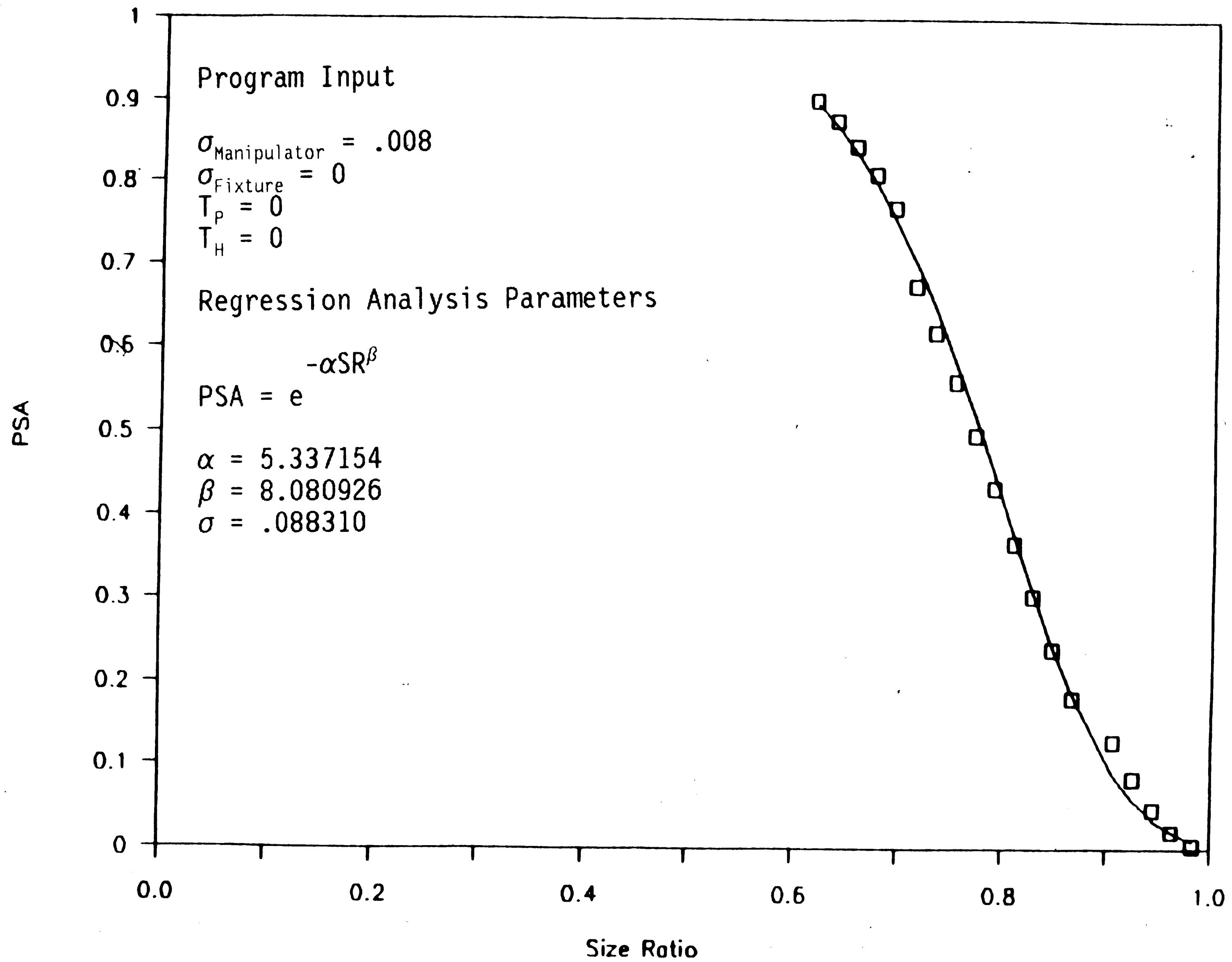
Figure 2. Theoretical and Regression Results

apparatus used in the experiment is shown in Fig. 3. A Selective Compliance Automatic Robotic Arm, SCARA class robot was used. Fixed rigidly to the end of the arm is a force/torque sensor. The sensor is capable of recording forces and torques along and about the X, Y, and Z axes. The robot is secured to the same precision machined as the fixture which contained the hole. The machine base also provided space for the serial monitors used to interface with the manipulator, the force/torque sensors and the printer.

A parallel gripper is attached to the force/torque sensor. The gripper is pneumatically operated and the input controlled using an air regulator. Figure 4 shows a detail view of the end of arm tooling including the fingers and pin. The pin location and repeatability is a critical factor in the experiment. The fingers had a .025 inch "V" shaped groove cut vertically into both the mating faces. The groove provided registration for the five different sized pins which were used to produce the different size ratios examined in the experiment. The pins are precision ground mold ejector pins. A commercially available precision drill gage is used to emulate the hole. Several hole diameters are provided on the gage.

Experimental Procedure

A simple robot motion program was written to simulate a pick-and-place operation of a manufacturing process where a pin is inserted into a housing. The communication between the robot and sensor controllers was developed to run automatically. The robot motion sequence is depicted and shown in Fig. 4 as:

1   Move to position C (gross movement)

2   Clamp gripper

3   Move to position B (gross movement)

4   Move to position D (gross movement)

5   Turn on force/torque output

6   Move to position A (fine movement)
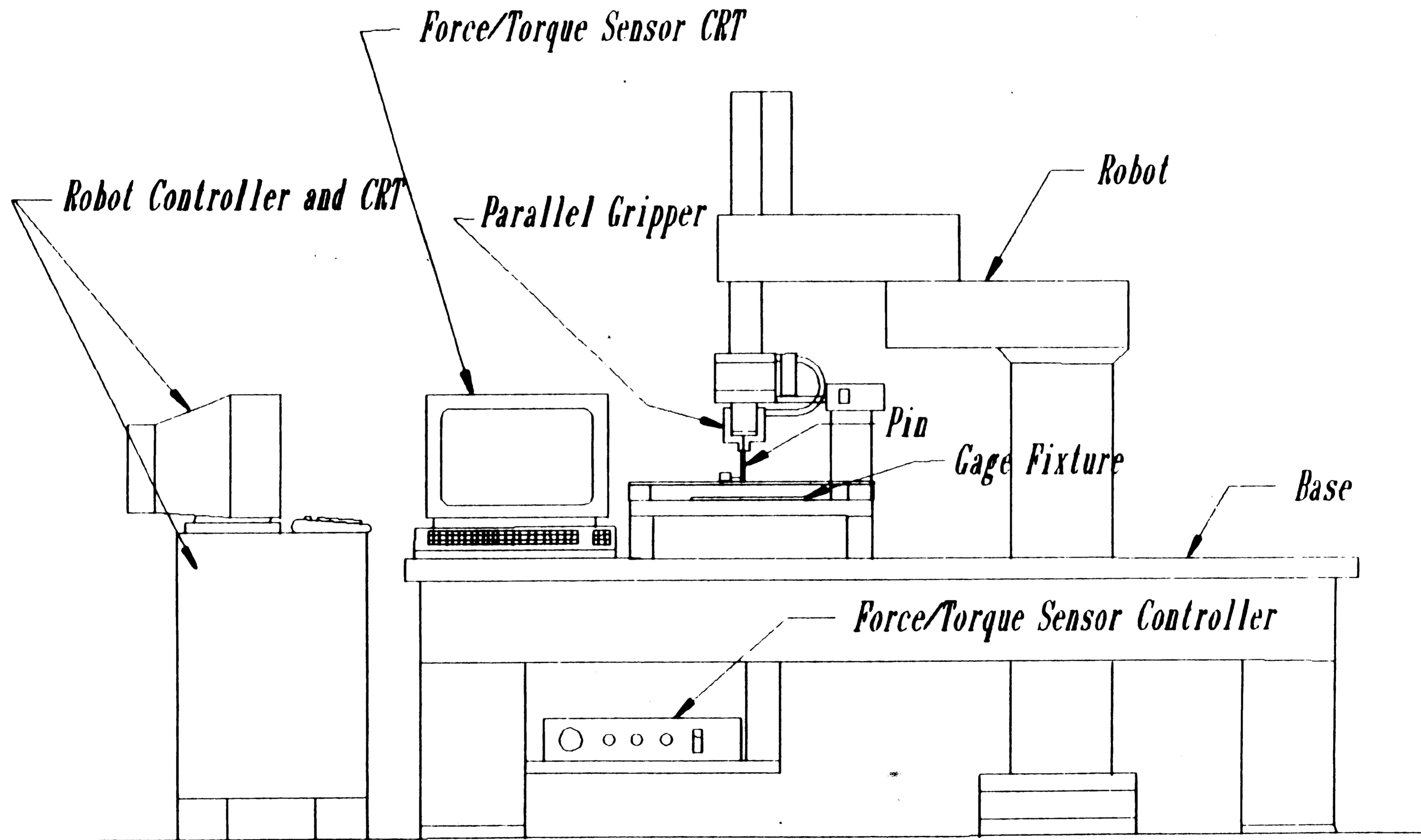
Figure 3. Experimental Apparatus

Location of Upper Scale

Manipulator

Force/Torque
Sensor

To Air Regulator

1.500   .062

12

2.625

Motion

Motion

B

C

Location of Lower Scale

Pin

1.450

Hole

D

Fixture/Housing

E

A
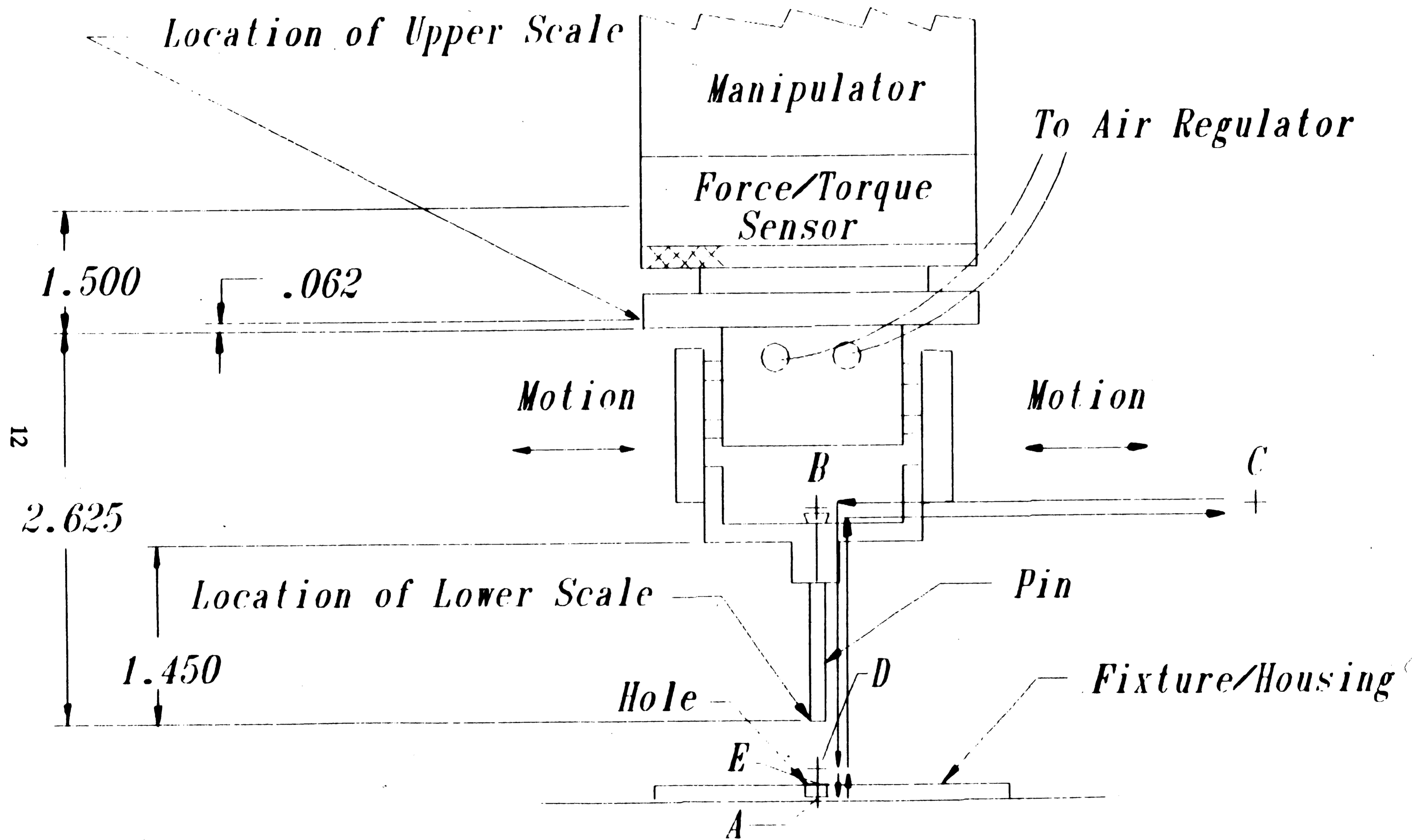
Figure 4. Detail of Robot End of Arm Tooling

7   Turn off force/torque output

8   Move to position D

9   Move to position B

10   Move to position C

11   End

   A pin and hole are selected. Their size ratio noted and the pin is loaded into the gripper. The robot is then jogged to a position where the pin centerline matched the hole centerline and the tip of the pin is exactly above the hole. This location is taught to the robot as position E. The X, and Y coordinates of position E are then transferred to the desired positions A, B and D. This aligns the four points in the Z direction allowing the robot to make a straight line move while attempting an insertion.

   To verify the results produced by the initial theory, as well as provide insight into less exact processing equipment, an artificial position error was implemented. The deviation to the exact insertion location in the X and Y directions was generated from a set of numbers having a normal distribution randomly generated by computer. The distribution had a mean of zero and standard deviation equal to .008 inches. This tolerance is typical of the stack-up found in an actual assembled product of four components. The tolerances and deviations are based on probable variations from specific datums which would be used to position the hole and to grip the pin. This distribution matched the input to the computer program that created the theoretical curve found in Fig. 1. The artificial error is added to positions A, B and D automatically when the program prompted the operator for an entry.

   The robot program was executed and a success or failure was determined and documented. If a failure occurred, the pin repositioned itself in the fingers because of a low air pressure setting in the gripper in which case it had to be manually replaced prior to the next insertion attempt. The low setting is necessary so that a catastrophic failure would not occur and detrimentally affect the force/torque sensor or the robot. Following a successful insertion the pin does not reposition itself

within the gripper. A new randomly determined error is input to the robot and the program continue to execute.

This procedure is repeated 300 times for size ratios .618, .708, .787, .865, .966, and 40 times for the remainder of the size ratios tested. The sample size is determined based on the confidence and reliability of the results desired. The sample size is calculated from:

$$R^n = 1.00 - C, \qquad (8)$$

where R is the estimated lower limit for reliability, n is the number of samples tested, and C is the confidence. For typical industrial applications the confidence level of 95% and the reliability of 99% is accepted. Substituting these values into the above equation results in a sample size of at least 298.

For each size ratio, the A, B, and D translations are modified through a manually taught location. This ensured that advantage is taken of the repeatability of the manipulator while minimizing the affect of robot inaccuracy. Although accuracy deviations for most industrial robots are far greater than repeatability variations most tasks in industry are taught making repeatability of prime importance.

Result of Experiment

Twenty different size ratios is used to generate the experimentally derived PSA curve. This should provide enough information to produce a reliable estimate of the PSA [14]. The communications baud rate between the devices is limited to 9600 reducing the resolution of the output recorded. Even at this relatively slow rate of data transmission the force/torque sensor had to be turned on and off during the cycle to allow the buffer to the monitor and printer to clear.

Figure 5 is a plot of Z axis force versus time for two different samples acquired from the force/torque sensor output. One curve was generated from a successful cycle while the other

Force/Torque Sensor Output

Time vs Z Axis Force
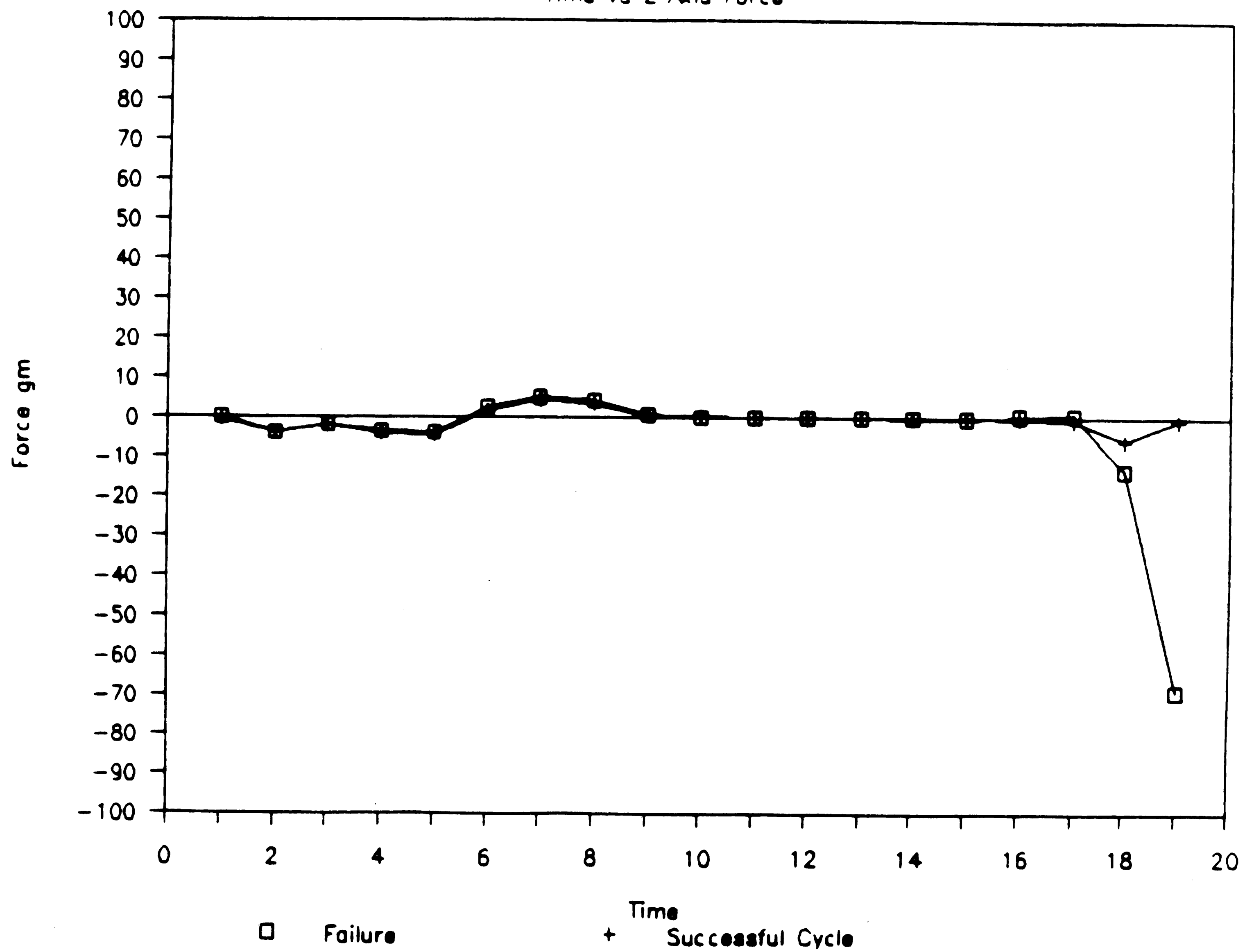
Figure 5. Force/Torque Sensor Force Outputs for a Successful and a Failed Insertion

profile is from a definite failure. The failed attempt is indicated by a large increase in the compressive force at the end of the cycle. The basic form of the two profiles demonstrates that the manipulator accelerates to constant velocity during the insertion cycle. As the robot accelerates the force/torque sensor observes a compressive force. During the period when the robot's acceleration reduces to zero to produce a constant velocity, the sensor observes a tensile force. This force is a result of the weight of the end of arm tooling.

Figure 6 shows time profiles of the X and Y axes torques generated from the force/torque sensor. The profiles are for a successful insertion cycle with no contact between the pin and hole. Noise at the beginning of the cycle is attributable to the rapid acceleration of the robot as it moves from point B and the mass of the end of arm tooling not being mounted exactly coincident with the axes of the sensor.

The torques shown in Fig. 7 are for a successful insertion when contact between the pin and hole is made. The Z axis force for this cycle would not indicate an appreciable increase in compression at the instant when contact is made. The increase in the X and Y axes torques verifies that contact has been made.

Figure 8 shows several different types of mating situations that the peg and hole can have. Figure 8a - 8d have no angular errors and Fig. 8e - 8h show the effect of angular error. The insertion defined by Fig. 7 corresponds to one of the angular error cases. The rigid insertion theory developed by Doydum would call such an insertion a failure. In actuality the robot is able to complete the insertion because the robot will respond to the forces and torques during by the mating of the pin and hole by moving so as to eliminate the angular misalignment.

Figure 9 is a graph of size ratio versus PSA for the data collected from the experiment. The graph is drawn to the same scale as that used in Fig. 1. Figure 9 also shows a curve resulting from fitting the experimental data to a Weibull curve using regression analysis methods similar to that used for the rigid model generated data presented earlier. The Weibull curve fits within the experimental error bound of each of the data points.

The Weibull curve fits for the experimental and theoretical PSA curves are shown in Fig. 10.
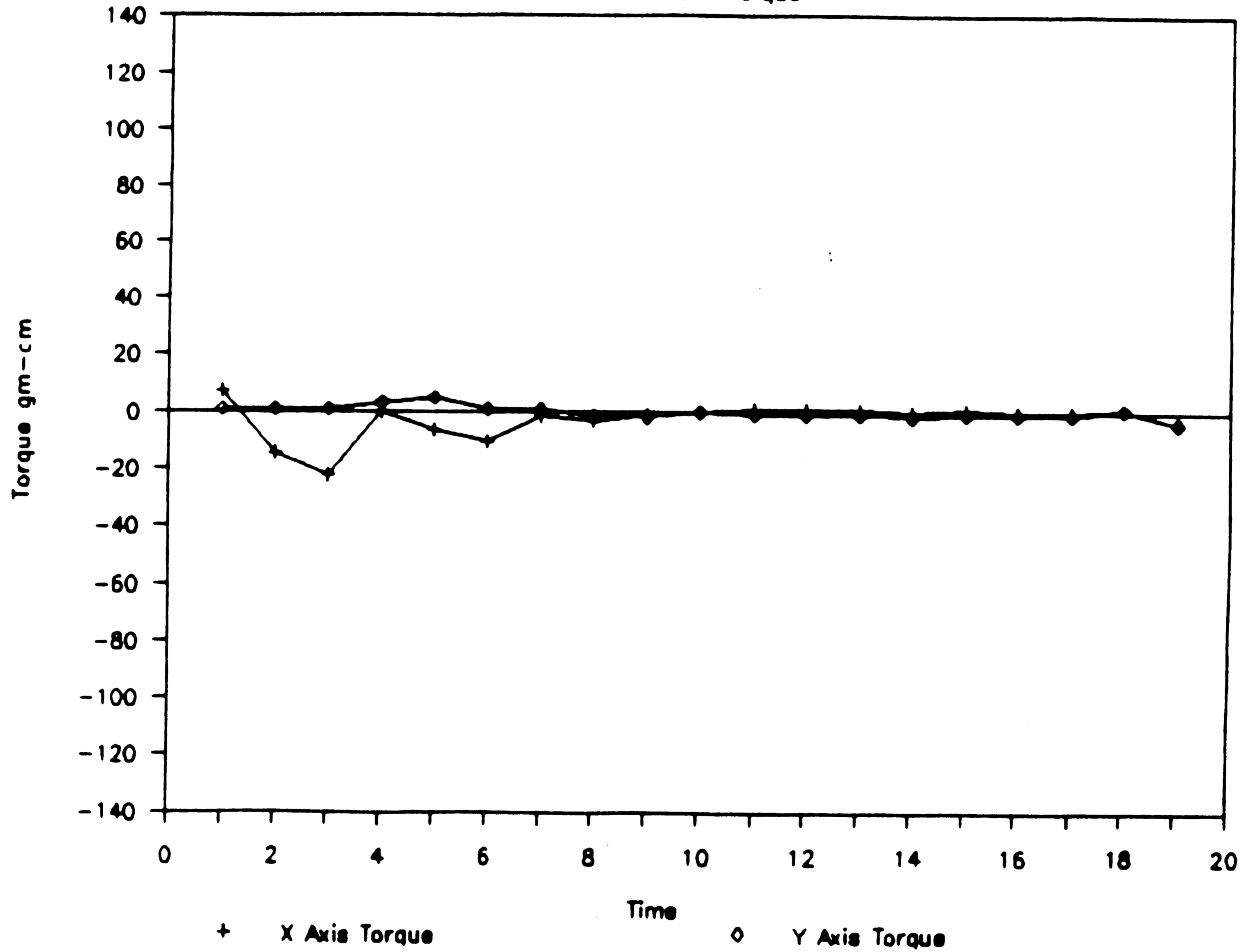
Figure 6. Force/Torque Sensor Torque Outputs for a Successful Cycle with no
Contact Between Pin and Hole
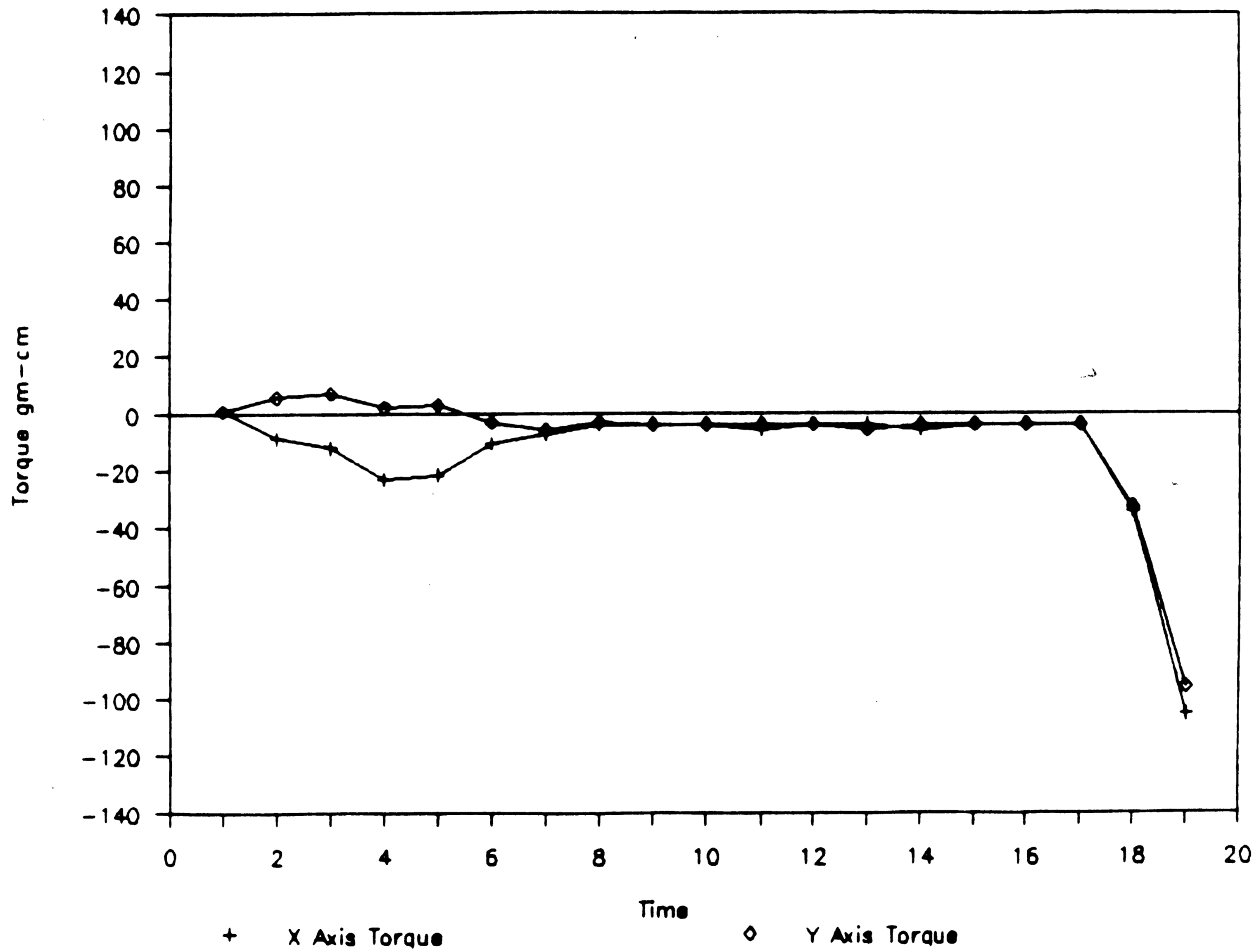
Figure 7. Force/Torque Sensor Torque Outputs for a Successful Cycle with Contact Between Pin and Hole
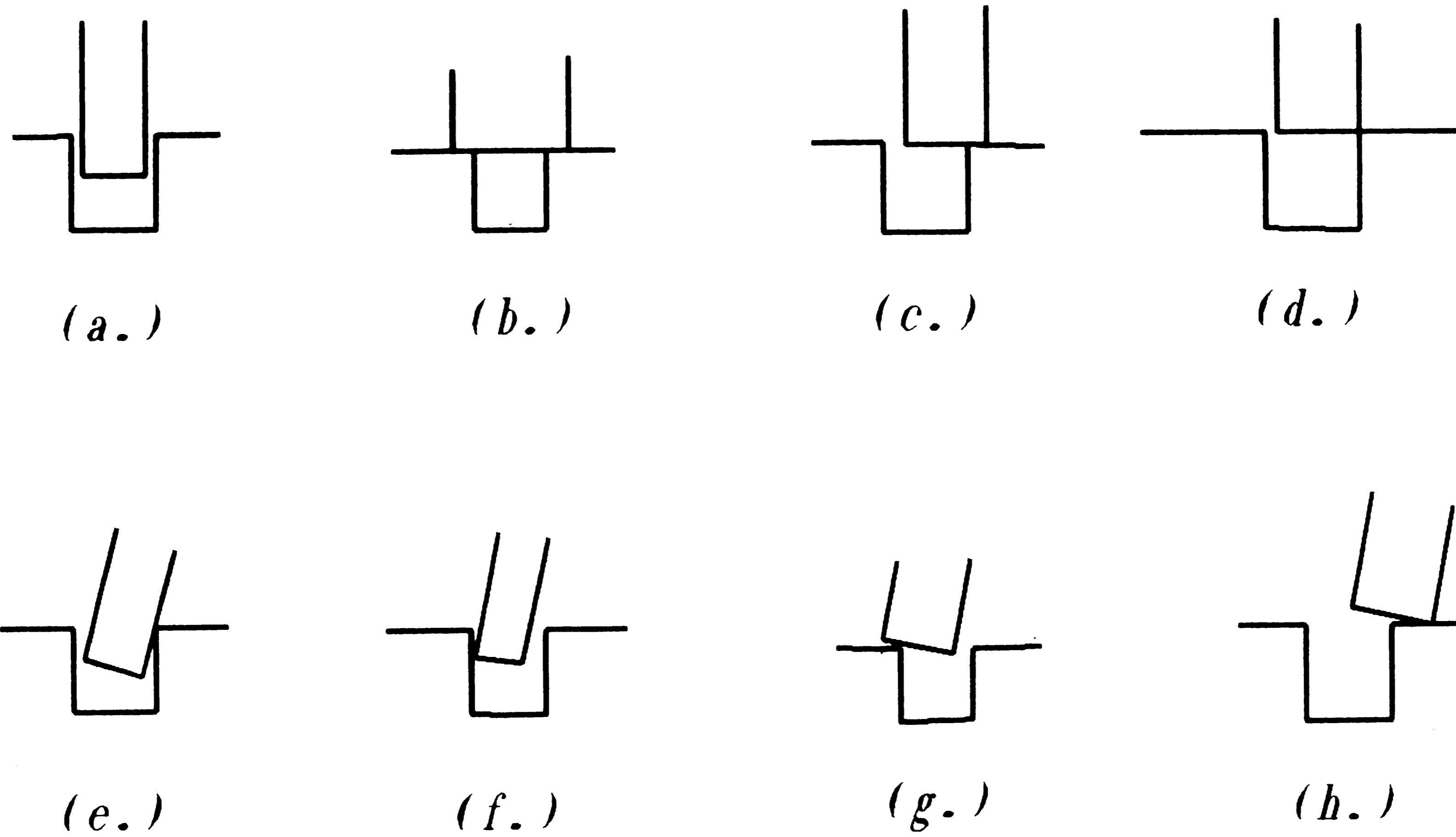
Figure 8. Mating Situations of a Pin and Hole

Experimental and Regression Results
Size Ratio vs PSA

Regression Analysis Parameters

$$PSA = e^{-\sigma SR^{\beta}}$$

α = 3.178071
β = 8.470402
σ = .268060

PSA
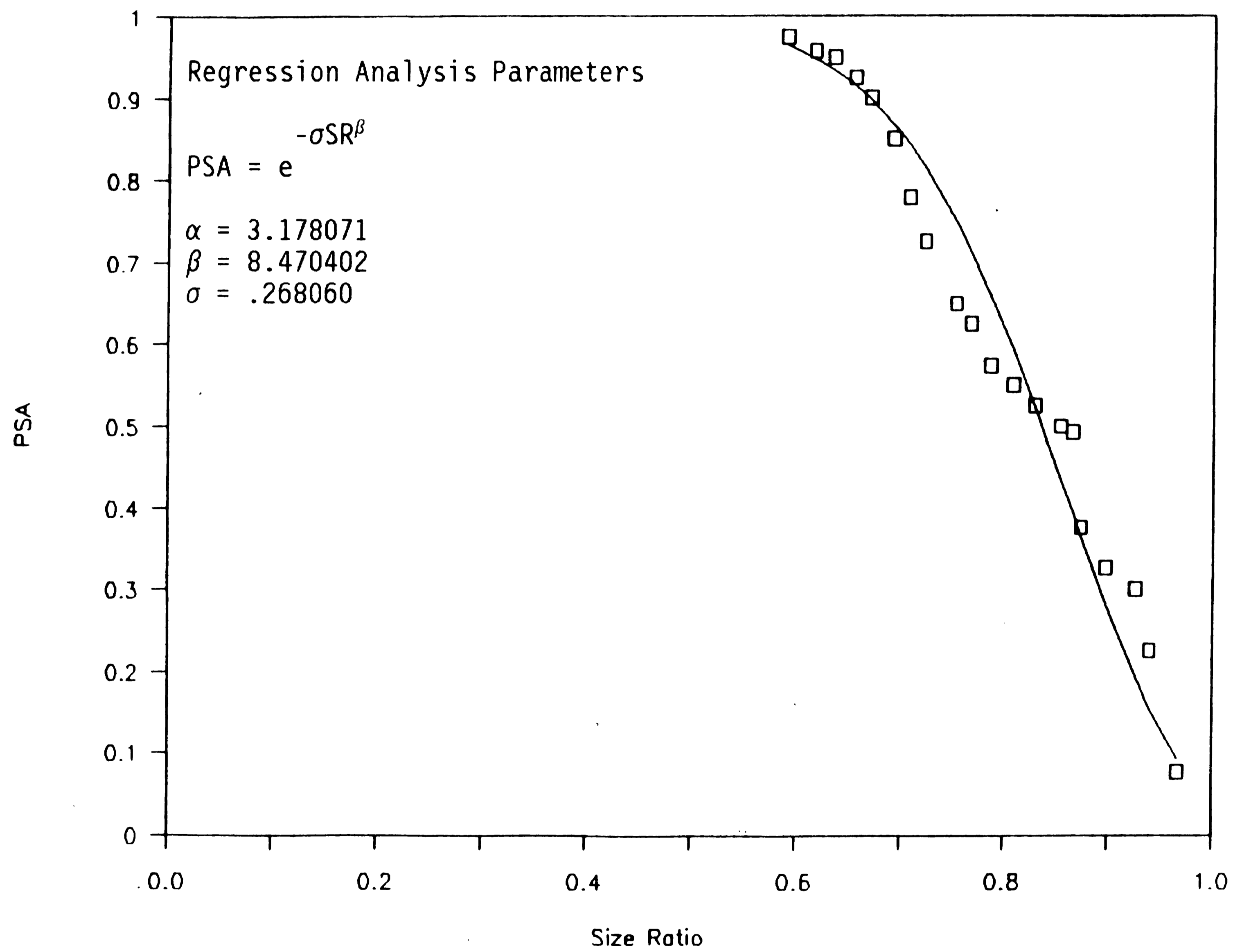
Size Ratio

Figure 9. Experimental and Regression Results

20

Comparisons of Experimental and Theoretical Regressions
Size Ratio vs PSA

Regression Analysis Parameters
Theoretical

$$PSA = e^{-\alpha SR^{\beta}}$$

α = 5.337154
β = 8.080926
σ = .088310

Regression Analysis Parameters
Experimental

$$PSA = e^{-\alpha SR^{\beta}}$$

α = 3.178071
β = 8.470402
σ = .268060

Experimental

Theoretical

PSA

Size Ratio

$SR_{eff.}$ 0.8 $SR_{act.}$
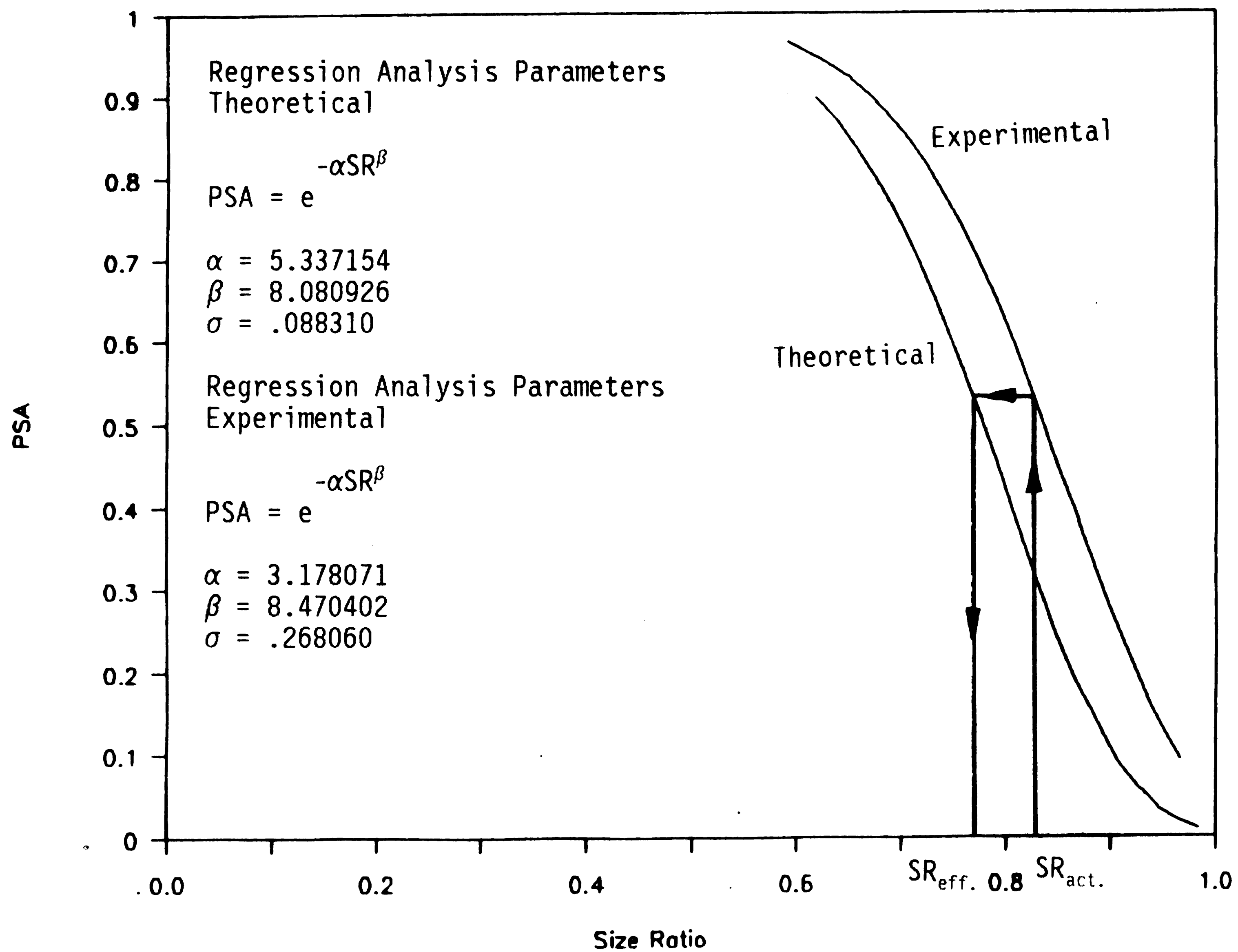
Figure 10. Comparisons of Regression Analysis Results on Experimental and Theoretical Data

For a given size ratio the experimental curve shows a significant increase in the PSA over that predicted in the theoretical curve. The plots appear to be parallel. The curves suggest that a smaller size ratio can produce better insertion efficiency than expected from the rigid system theory.

The effective size ratio, $SR_{eff.}$, is the size ratio that would make the rigid insertion model PSA equal to the experimental PSA. The experimental PSA value being at the actual size ratio, $SR_{act.}$. The effective size ratio is plotted against the actual size ratio in Figure 11. The curve is determined by noting that for the PSA's to be equal the two Weibull models must be related so that:

$$R_{eff.} = [\ \alpha_{act.}/\alpha_{eff.}\ ]^{1/\beta_{eff.}} \times R_{act.}^{(\beta_{act.}/\beta_{eff.})} \tag{9}$$

Figure 11 suggests that the effective size ratio increases linearly with the actual size ratio. A linear regression results in a simple and highly accurate relationship between the actual and effective size ratio.

$$R_{eff.} = .970977\ R_{act.} - .03416 \tag{10}$$

The difference between the effective and actual size ratio is interpreted as an increase in the effective size of the hole. The hole size correction is the change from the actual hole diameter to a new diameter that would yield the effective size ratio. Figure 12 shows the resulting hole size correction per mean hole diameter as the actual pin to hole size ratio varies. The curve is calculated using:

$$\frac{\delta H}{d_p} = \frac{.029023\ SR_{act.} + .03416}{SR_{act.}(.970977\ SR_{act.} - .03416)} \tag{11}$$

where H is the difference in the hole size required. The curve illustrates that increasing the size ratio or decreasing the assembly clearance decreases the dimensionless hole size correction. This implies that the allowable misalignment angle between the pin and the hole, α, must decrease as

Effective Size Ratio Calculated from Experimental to Theoretical

$$SR_{eff.} = [\alpha_{act.}/\alpha_{eff.}]^{1/\beta_{eff.}} \times SR_{act.}^{(\beta_{act.}/\beta_{eff.})}$$

$SR_{eff.} = .970977\ SR_{act.} - .03416$

$\sigma = .000355$

if $SR_{eff.} = 1$, $SR_{act.} = 1.065079$

Effective Size Ratio

Actual Size Ratio

23
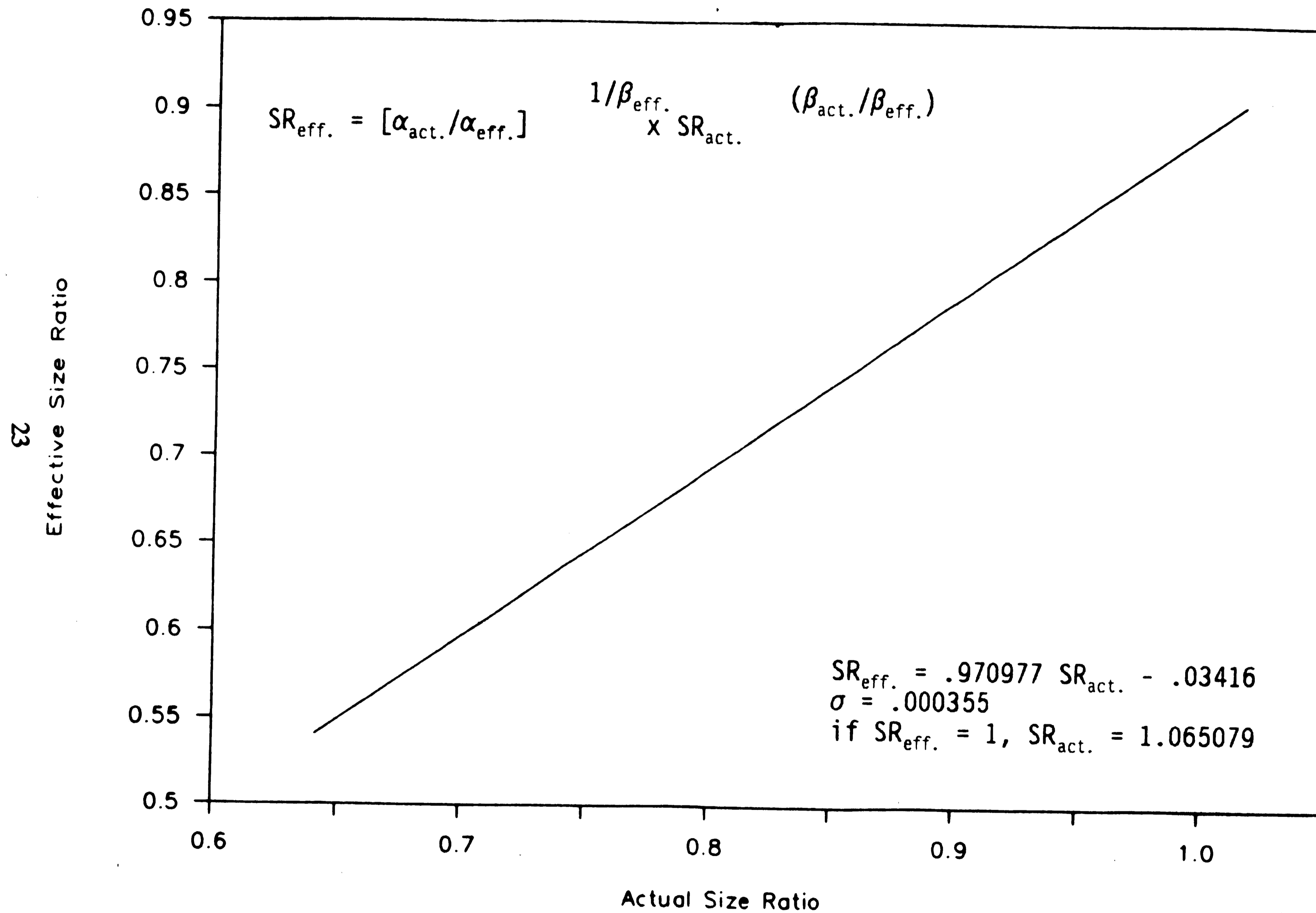
Figure 11. Effective Size Ratio Calculated from Experimental to Theoretical

Dimensionless Hole Size Correction

$$\frac{\delta H}{d_P} = \frac{.029023\ SR_{act.} + .03416}{SR_{act.}(.970977\ SR_{act.} - .03416)}$$
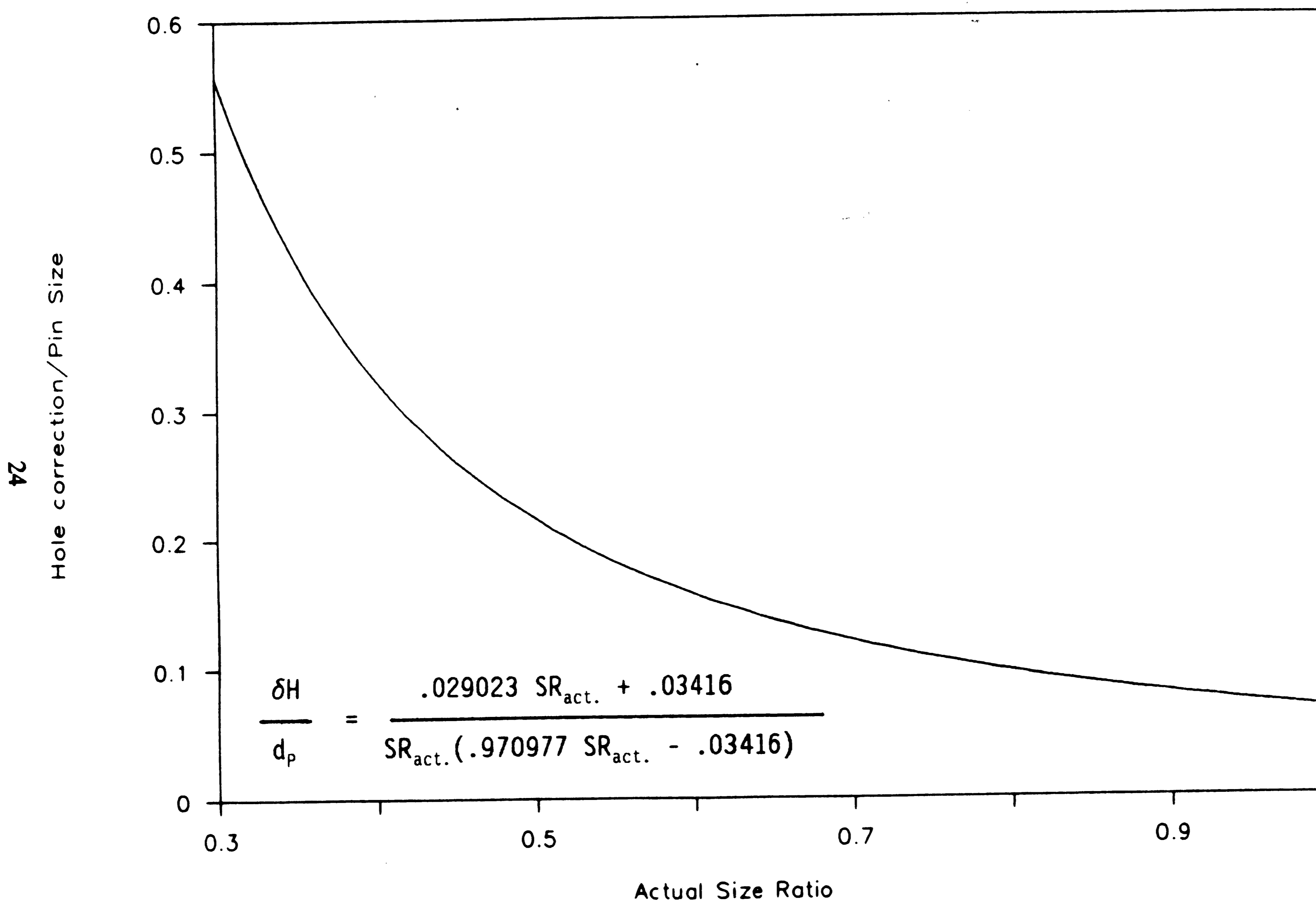
Figure 12. Dimensionless Hole Size Correction

the size ratio gets larger for a successful assembly to occur.

The experimentally generated results show that the rigid insertion theory is too conservative if one assumes that contact between mating components does not affect the quality of the end product as long as the insertion is completed. The error between the experiment and rigid theory is easily explained by angular misalignment. It is well known that some degree of angular misalignment is allowed in compliant insertion [15]. We now propose and experimentally validate a modification to the above theory to incorporate the angular and linear compliance within the manipulator/gripper, fixture and component parts to form a compliant insertion model.

CHAPTER 3

COMPLIANT INSERTION MODEL

Introduction

The rigid theory uses as an insertion failure criteria the occurrence of contact between the bottom of the pin and the top of the surface surrounding the hole. It assumes that the hole and pin axes are parallel. The criteria does not reflect a typical insertion process because of angular misalignment and system compliance. The experimental results for a given size ratio show a consistent increase in the percent of successful assemblies over the theoretical results. This implies that the peg can be successfully inserted into the hole when contact during mating occurs as shown in Fig. 8.

The insertion failure criteria is modified in the following theory to allow contact between the pin and hole as long as the insertion is completed. This is accomplished by incorporating compliance in the effective size ratio model. This is rationalized by two arguments; every mechanism has some amount of inherent compliance, and contact between mating components during the insertion does not necessarily diminish the quality of the assembly.

Compliant Hole Size

The compliant hole size incorporates the effect of system compliance. The model is based on the free-body diagram shown in Fig. 13 where the X,Y and Z axes are orthogonal, the X,Y plane is horizontal and the Z direction is vertical; the positive Z direction pointing down. The displacements are defined as:

α = Angular displacement of the pin about ot's base.

X_T = Total pin tip displacement in the XY plane.

X_C = Displacement of the base of the pin parallel to the XY plane.

X_R = Displacement of the pin about it's base due to rotation about the Y axis.
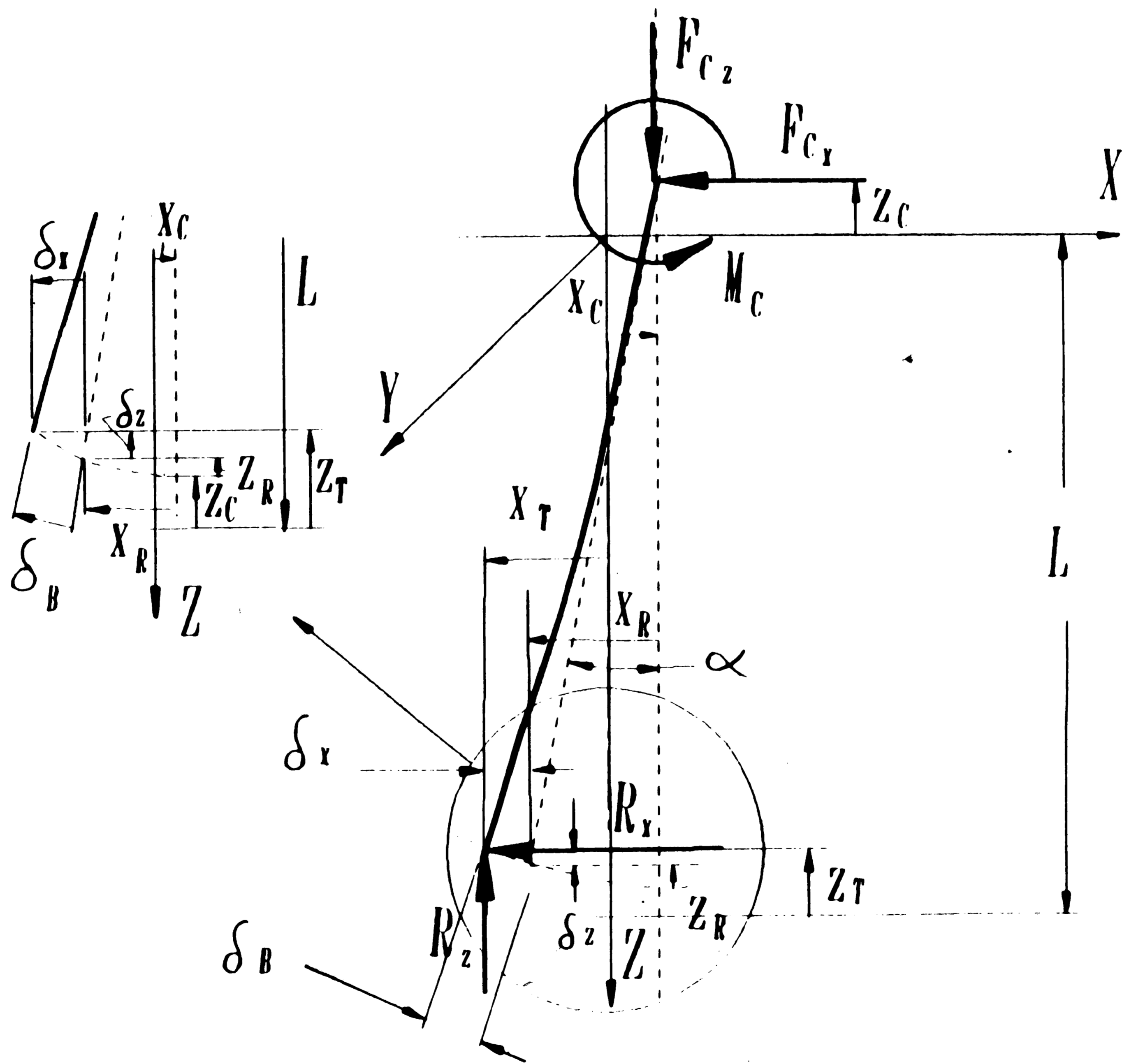
Figure 13. Compliance Model Free-Body Diagram

δ_x = Displacement of the in the XY plane due to bending.

Z_T = Total pin tip displacement in the Z direction.

Z_C = Displacement of the base of the in the Z direction.

Z_R = Displacement of the pin about it's base due to rotation about the Y axis.

δ_z = Displacement in the Z direction due to bending.

δ_B = Total displacement of the pin due to bending.

The forces and moments are defined as:

R_X = Reaction force on the pin in the X direction caused by the hole.

R_Z = Reaction force on the pin in the Z direction caused by the hole.

M_C = Rotational moment at the base of the pin.

F_{Cx} = Force parallel to the XY plane at the base of the pin.

F_{Cz} = Force in the Z direction at the base of the pin.

F_B = Internal pin forces.

F_{Bx} = Internal pin forces parallel to the XY plane.

F_{Bz} = Internal force in the Z direction.

The compliance model requires the use of the following system stiffnesses:

K_{CT} = Stiffness of the gripper/manipulator in the XY plane.

K_{Cz} = Stiffness of the gripper/manipulator in the Z direction.

K_R = Rotational stiffness of the gripper/manipulator.

K_B = Stiffness of the pin.

We assume that the system is in static equilibrium and the X and Y axes are oriented (with no loss in generality) so that all translations are in the X and Z directions and all rotations are about the Y axis. Simple kinetics gives the force exerted on the pin in the X and Z directions as

$$\Sigma \ F_X \ = \ 0 \quad + \rightarrow$$

(12a)

28

$$-F_{Cx} = R_x$$

$$\Sigma \ F_z = 0 \quad + \downarrow$$

$$F_{Cz} = R_z \tag{12b}$$

while the moment on the pin is

$$\Sigma \ M_y = 0$$

$$M_C = R_x Z_T + R_z X_T \tag{12c}$$

Kinematics results in

$$X_T = X_C - X_R - \delta_x \tag{13a}$$

$$Z_T = Z_C + Z_R + \delta_z \tag{13b}$$

and from geometry we note,

$$X_R = L \sin \alpha$$

$$Z_R = L \cos \alpha$$

$$\delta_x = \delta_B \cos \alpha \tag{14}$$

$$\delta_z = \delta_B \sin \alpha$$

Substituting Eqs. (14) into (13) we obtain

$$X_T = X_C - L \sin \alpha - \delta_B \cos \alpha \tag{15a}$$

$$Z_T = Z_C + L (1 - \cos \alpha) + \delta_B \sin \alpha \tag{15b}$$

The displacements are related to the forces through the constitutive stiffness equations. The XY planar, Z axis translational and rotational, and bending stiffness equations being, respectively,

$$F_{Cx} = K_{Cx} X_C \tag{16a}$$

29

$$F_{Cz} = K_{Cz}Z_C \tag{16b}$$

$$M_C = K_R\alpha \tag{16c}$$

$$F_B = K_B\delta_B \tag{16d}$$

The stiffnesses K_{Cx}, K_{Cz} and K_R are determined experimentally. The stiffness of the pin, K_B, is determined by assuming it to be a cantilevered beam. Thus

$$K_B = \frac{F_B}{\delta_B} = \frac{3EI}{L^3} \tag{17}$$

Substituting Eqs. (14a), (14c), (16a) and (16c) into Eq. (15a) yields

$$X_T = \frac{F_{Cx}}{K_{Cx}} - L \sin \alpha - \frac{F_B}{K_B} \cos \alpha \tag{18}$$

We eliminate the internal bending force in Eq. (18) by noting from Fig. 13 that

$$F_B = R_X \cos \alpha + R_Z \sin \alpha \tag{19}$$

Substituting Eqs. (12a), (12b) and (19) into Eq. (18) yields

$$X_T = \frac{F_{Cx}}{K_{Cx}} - L \sin \alpha + \frac{F_{Cx}}{K_B} \cos^2 \alpha - \frac{F_{Cz}}{K_B} \sin \alpha \cos \alpha \tag{20}$$

When α is very small

$$\sin \alpha \approx \alpha \tag{21a}$$

and

$$\cos^2 \alpha = 1 - \sin^2 \alpha = 1 - \alpha^2 \tag{21b}$$

Substituting Eqs. (16c) and (21) into Eq. (20) yields

$$X_T = \left[\frac{F_{Cx}}{K_{Cx}}\right] - \left[L \ \frac{M_C}{K_R}\right] + \left[\frac{F_{Cx}}{K_B}\left(1 - \frac{M_C^2}{K_R^2}\right) - \left[\left(\frac{F_{Cx}}{K_B}\right)\left(\frac{M_C}{K_R}\right)\left(1 - \frac{M_C^2}{K_R^2}\right)\right]\right]^{1/2} \quad (22)$$

This is the total XY plane directional displacement of the tip of the pin due to the rotational and planar compliance of the pin/gripper/manipulator system.

The displacement X_T found in Eq. (12) is equivalent to the modification required in the hole size, δH, identified in Eq. (11). When added to the actual hole diameter the effective hole diameter is determined. The effective size ratio where;

$$SR_{max} = \frac{(d_h + \delta H) + (T_h - T_p) - 2 \ [(F_x^2 - M_x^2) + (F_y^2 - M_y^2)]^{1/2}}{d_h + \delta H} \quad (23)$$

The effectiveness of this model is verified below.

The preceding derivation requires knowledge of the system stiffness. An experiment was designed to obtain the force, moment and displacement data required to compute it.

Experimental Procedure

The compliance experiment requires obtaining both displacement and force data. The setup is shown in Fig. 14. It consists of a SCARA class manipulator, a four place digital indicator and a precision vernier gage. The digital indicator is mounted to the base plate and contacts the manipulator 1.437 inches below the force/torque sensor on the head of the arm. The precision vernier gage is positioned to contact the tip of the pin as it applies a constant force. The force/torque sensor is located on the head of the robot. It's output is routed directly into a serial monitor for instantaneous viewing.

The manipulator head is positioned at the same location during the first experiment. This point is labelled the zero degree position. The output of the force/torque sensor is turned on and the

31

Air Regulator

Force/Torque
Sensor

Upper Indicator

Mounting

Parallel
Gripper

Fingers

Pin
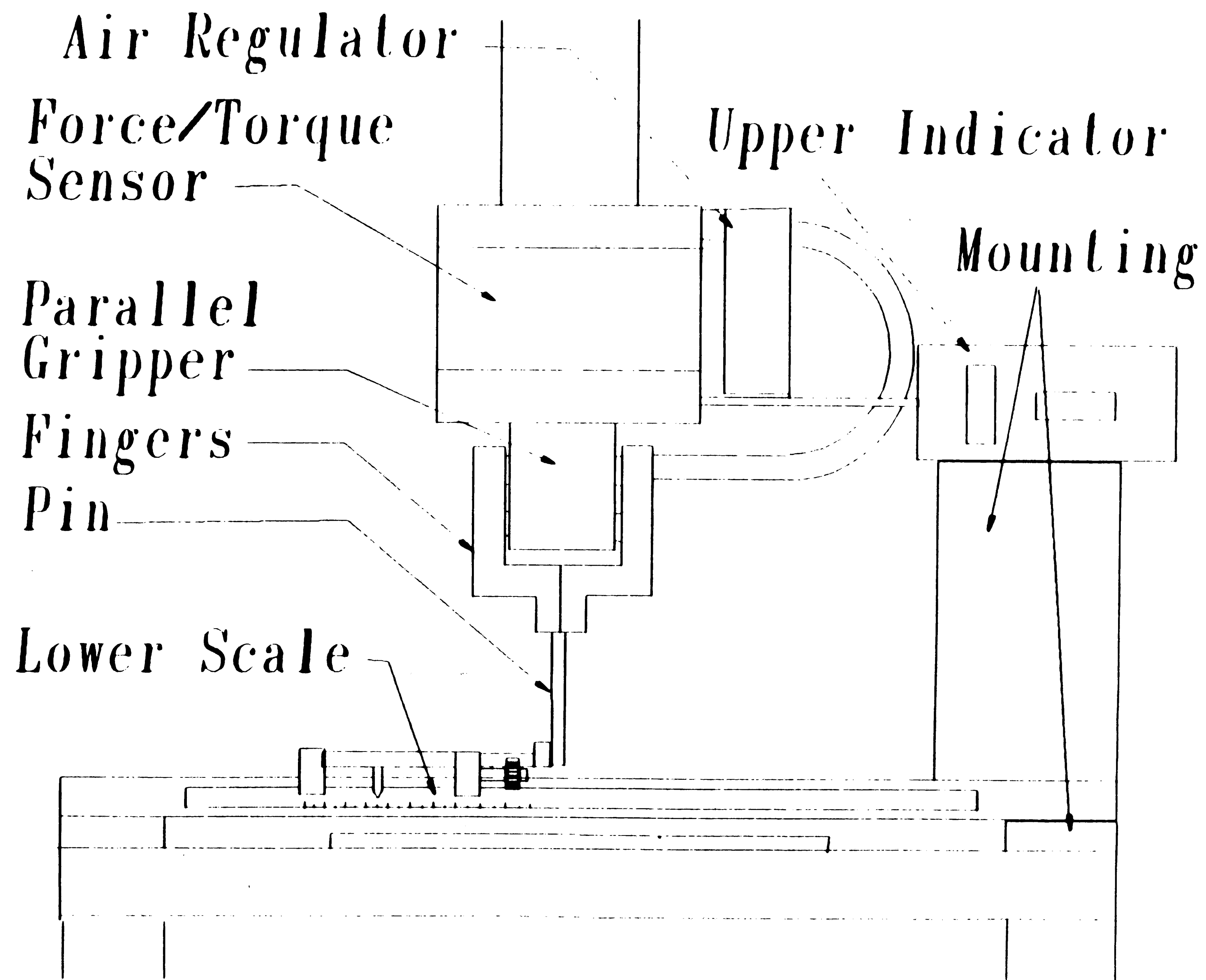
Lower Scale

Figure 14. Displacement Measurement System

lower displacement vernier scale is positioned to contact the pin without imparting any change in the output of the sensor. The digital or upper displacement scale and lower scale reading is then recorded. The vernier is displaced causing a change in the output of the force/torque sensor and in both the upper and lower scales. All readings are recorded. This process is repeated for ten increasing vernier values.

The manipulator head is then rotated approximately 45 degrees, the displacement scales and force/torque sensor are zeroed, and the procedure repeated. The robot head is rotated in approximately 45 degree increments from 0 to 315 degrees providing data from a total of eight angles.

Experimental Results

<u>Resulting Displacements.</u>   Figure 15 shows a graphical representation of the linear displacements at the upper indicator position versus angle. Rotational displacements of the pin are determined by taking the difference between the changes in the upper and lower scales and dividing by the distance between the gages, 2.687 inches. The corresponding angles are plotted in Fig. 16. The raw data for both linear gages is also given in Table 2 of the appendix with all of the other raw data collected in this experiment.

<u>Force/Torque Results.</u> The raw force data taken at eight angular orientations and nine force levels is shown in Fig. 17. The plot gives a top view of the force profile recorded by the sensor. A schematic representation of the gripper is superposed to indicate the direction the robot head is pointing when the experiment is conducted. The test angles are approximately 45 degrees from each another. The raw force data is adjusted to compensate for slight differences in angle and replotted in Fig. 18. The force data is then scaled using one unit force output equals .20 grams [16].

The raw torque data is shown in Fig. 19. A schematic representation of the gripper indicates the approximate robot direction during experiment. The torques are gathered simultaneously with the forces. The moments are adjusted in the same manner as the forces to compensate for any
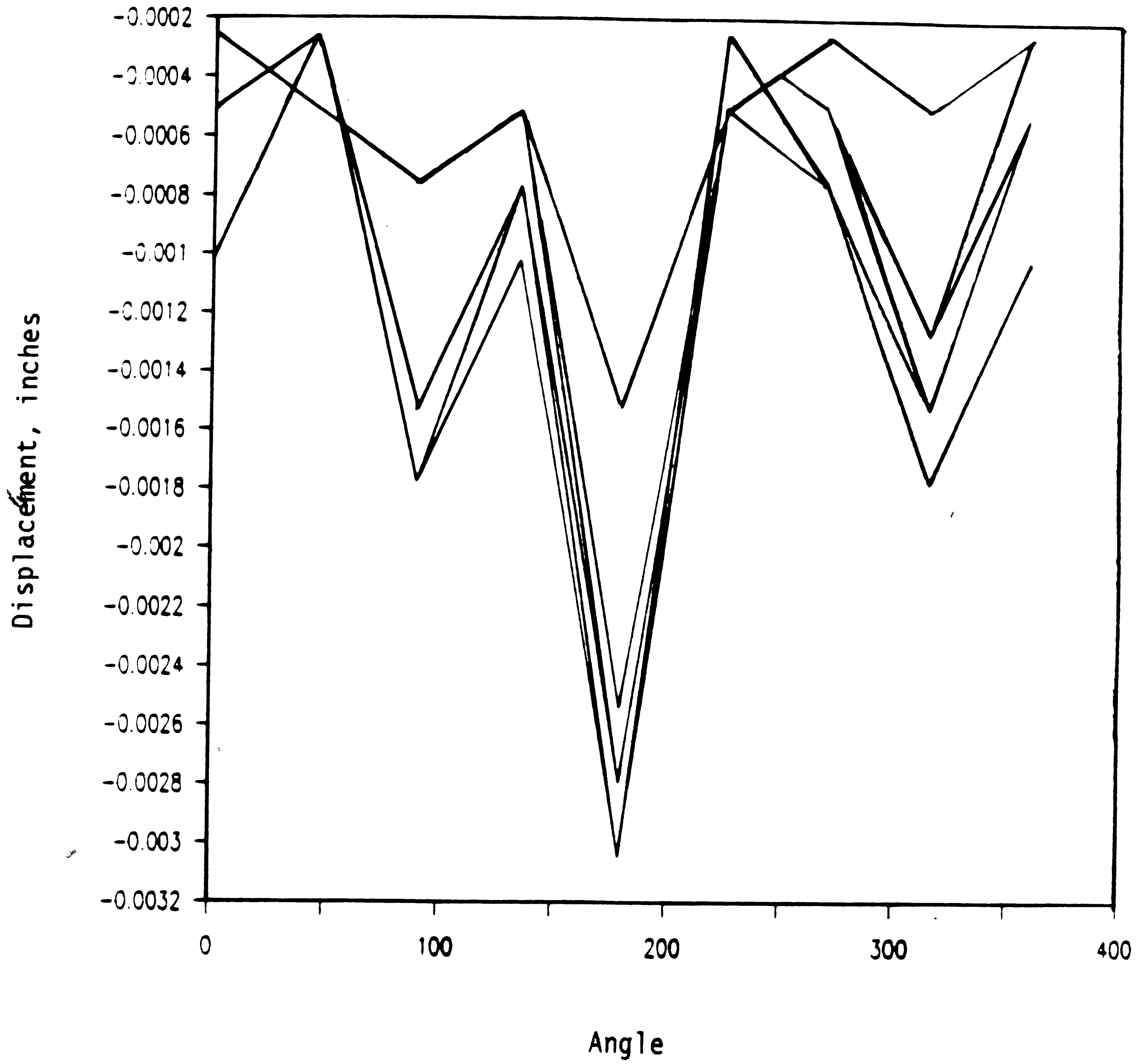
Figure 15. Upper Displacements

34
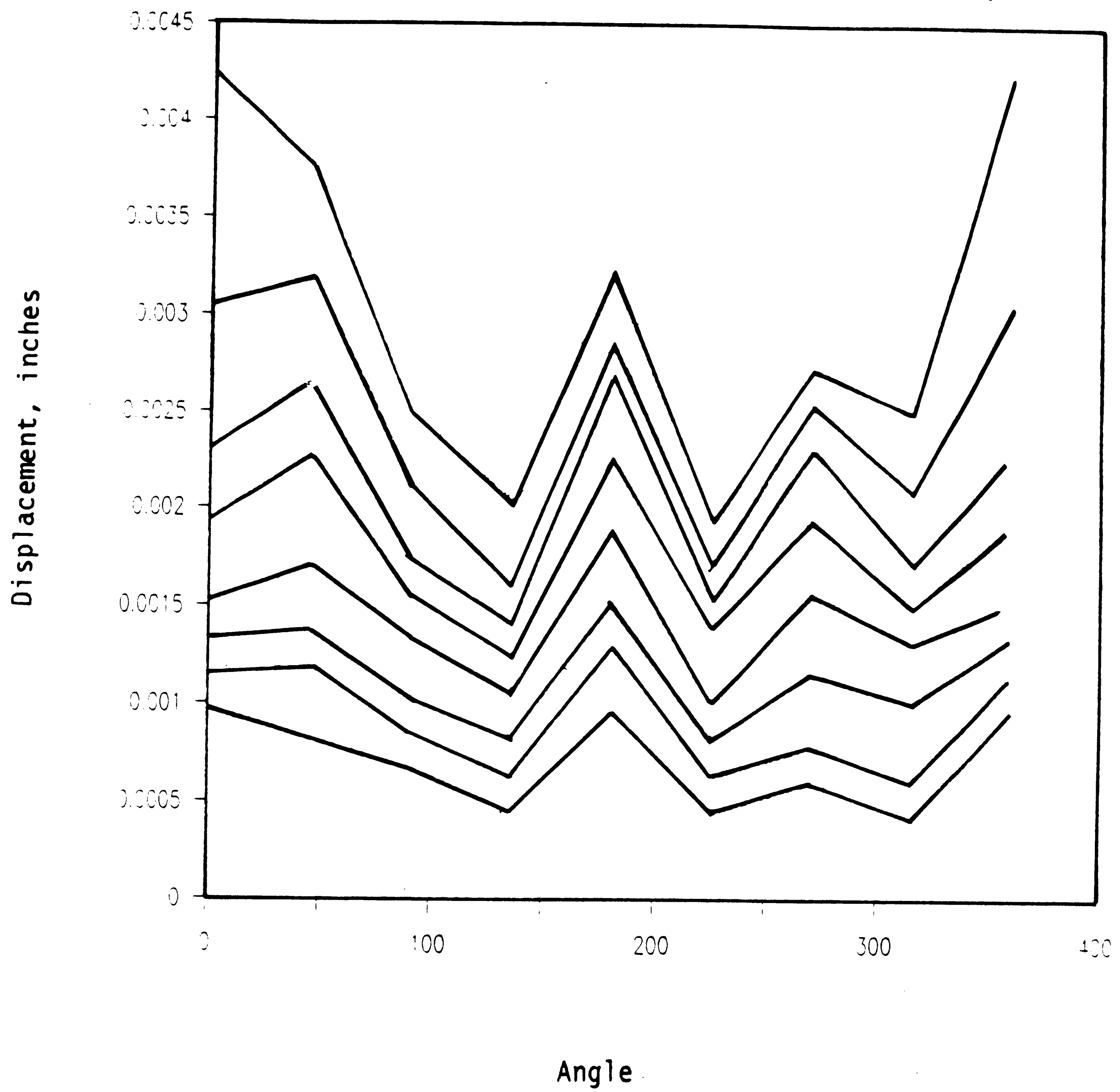
Figure 16. Lower Displacements
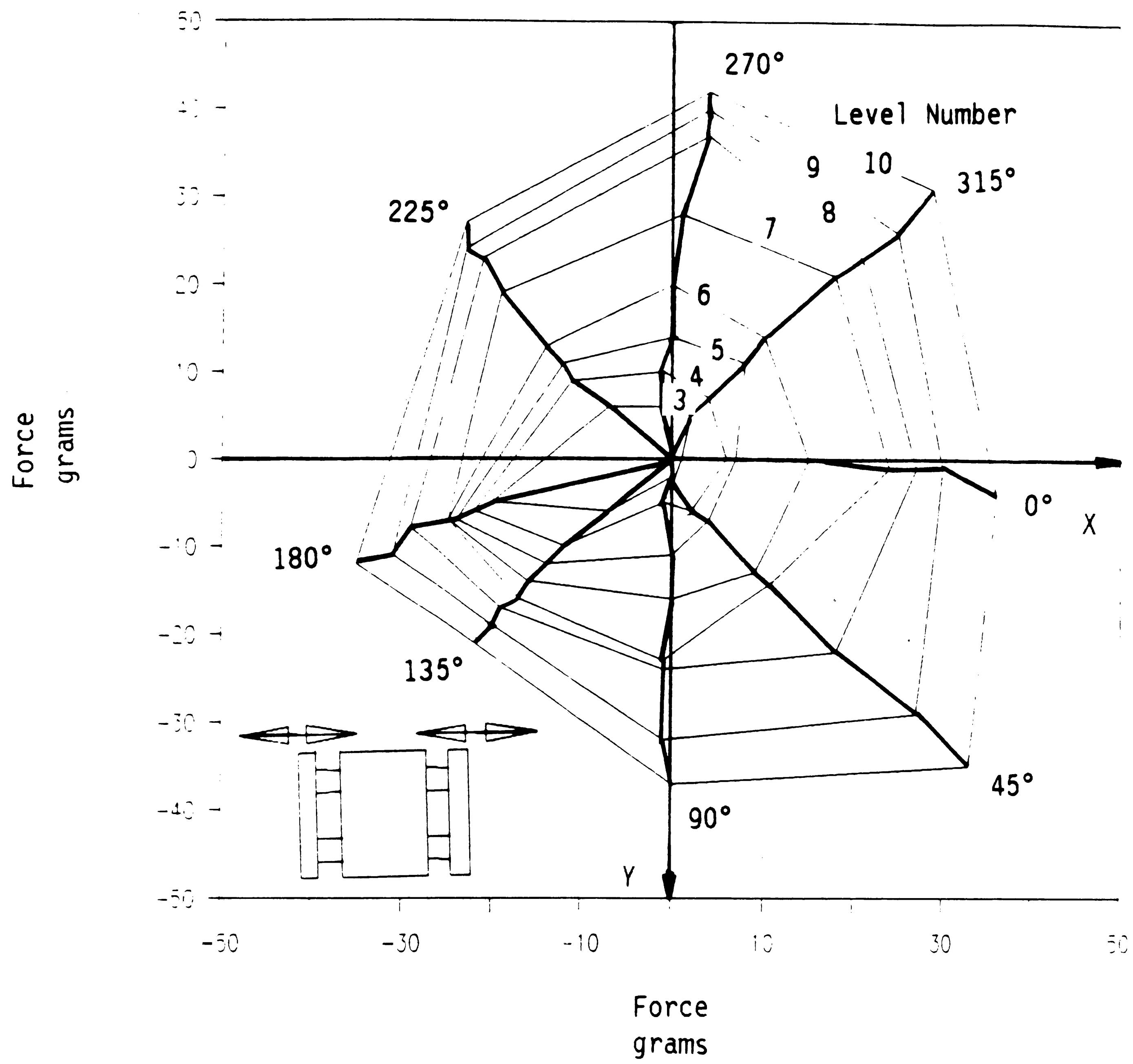
Figure 17. Raw Force Data
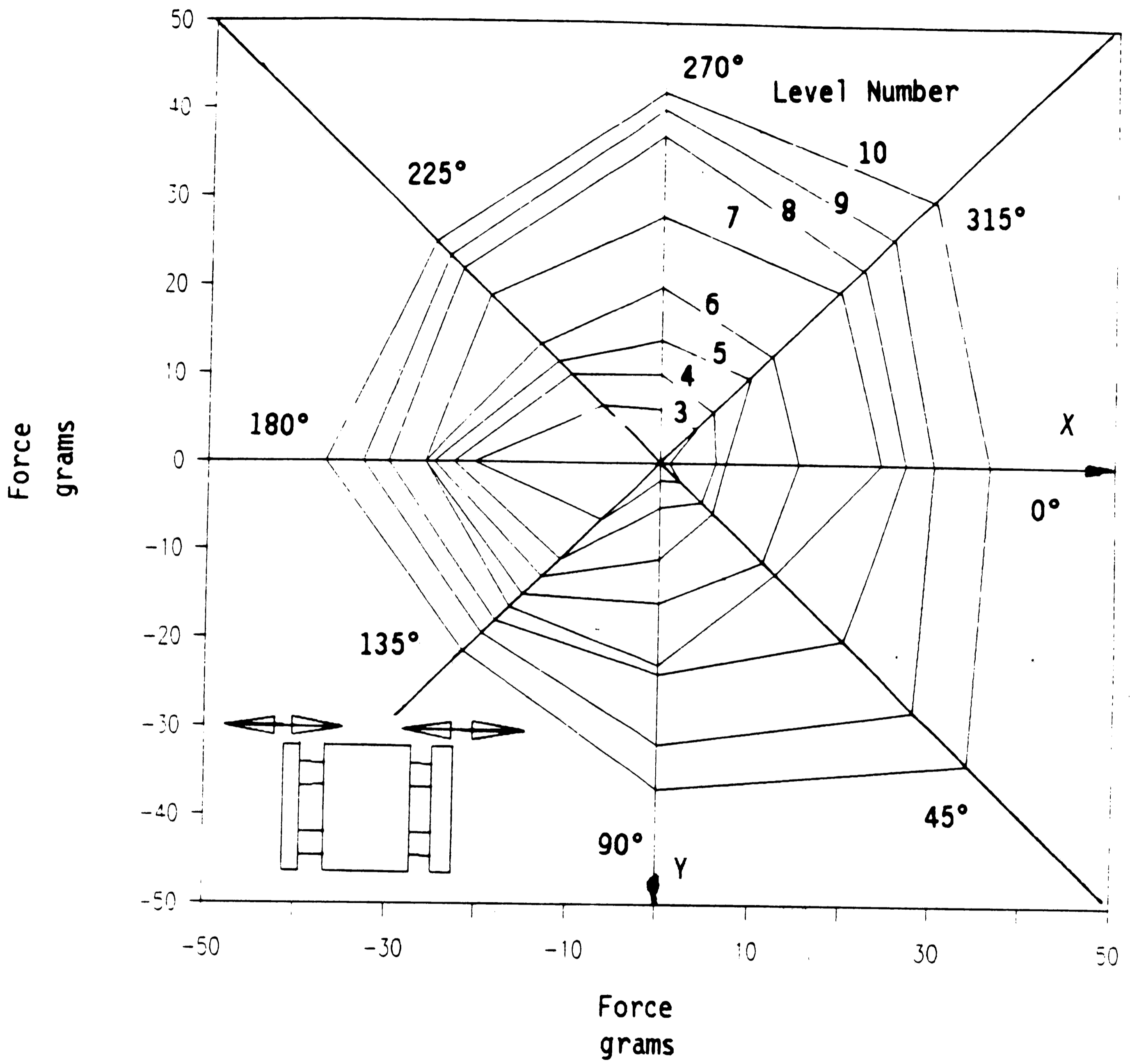
Figure 18. Adjusted Force Data

37

angular differences, and are plotted in Fig. 20. The torque data is then scaled using one unit torque output equals .80 gm-cm.

Figures 17 through 21 show force and torque data at the force/torque sensor. The data is the moved to the upper displacement indicator location by a simple transformation depicted in Fig. 21. The sensor data is moved along the positive Z axis by a distance $d1 = 1.437$ inches as shown in Fig. 4. The transformed moments due to the X and Y forces are added to the measured moments to provide the total X and Y direction moments as shown in Fig. 22. The X and Y directions in this figure refer to the X and Y directions of the induced displacement.

System Stiffness

The effective size ratio is dependent on the stiffness of the system. The stiffness is calculated from raw data using Eqs. (16). In the stiffness experiments the robot head is rotated so that contact is made by the pin with the sides of the hole from various directions. In the insertion experiment such contacts occur although no rotation is made. Figure 23 shows a contour plot of the linear stiffness. A clearer depiction of the stiffness is obtained by rotating it about the Z axis by a 45 degrees. This rotation fixes the stiffness relative to the base of the robot in a manner similar to that during the insertion experiment. The rotated view is shown in Fig. 24. A schematic representation of the gripper is superimposed for clarification.

The displacements used to obtain these stiffnesses are of the same order of magnitude as the accuracy of the upper displacement indicator. Although this produces linear stiffness errors as great as 50%, as we later show the linear stiffnesses are so much greater than the rotational stiffnesses as to not be significant.

The bulk of the compliance within the system is due to the angular displacement at the head of the manipulator. Angular stiffness contours are given in Fig. 25. The rotational stiffness system is transformed in a manner similar to the linear stiffness and the results are shown in Fig. 26. The displacement due to rotational compliance is an order of magnitude larger than that for the planar compliance and was measured by a comparably accurate lower displacement indicator.
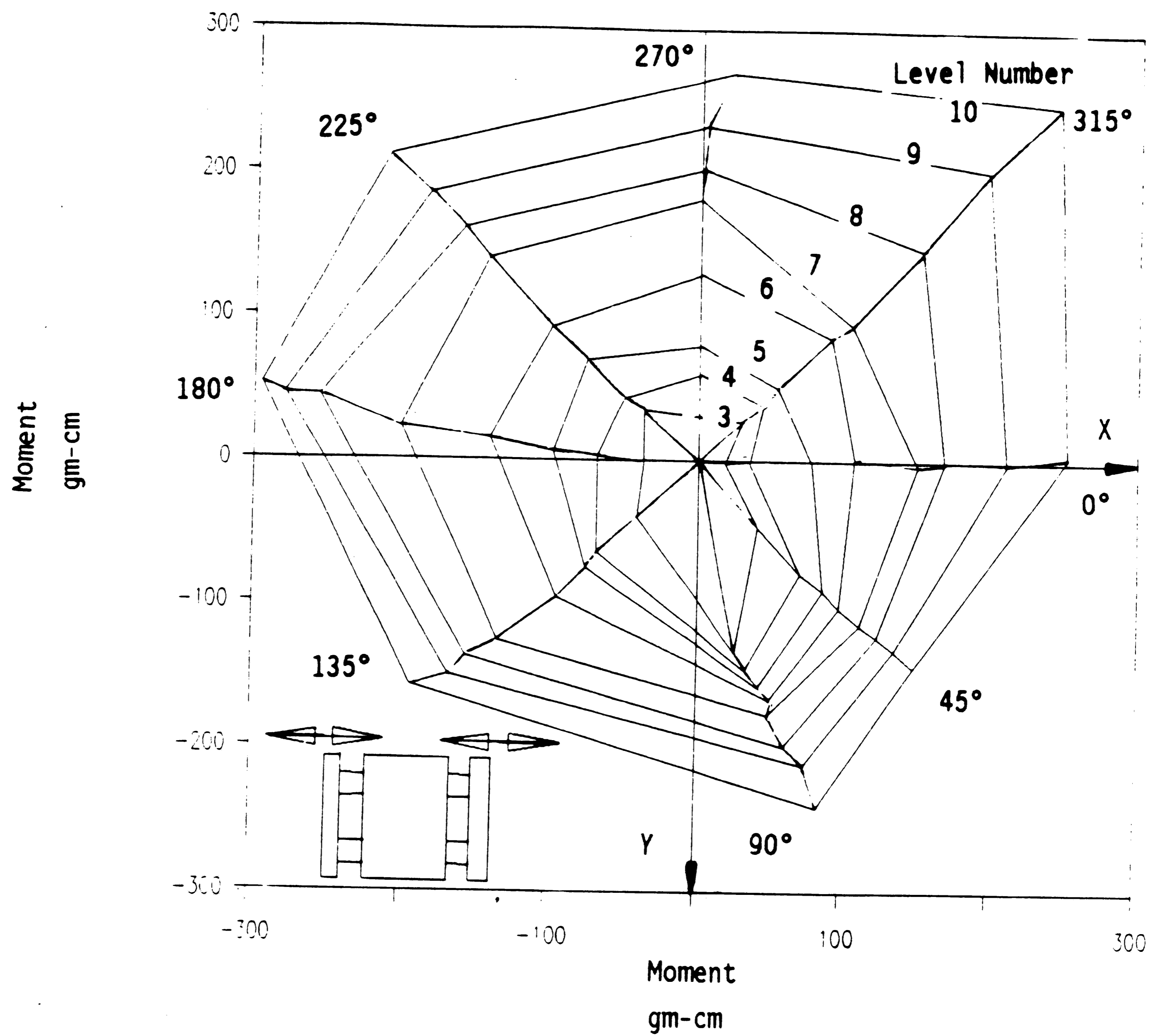
Figure 19. Raw Moment Data
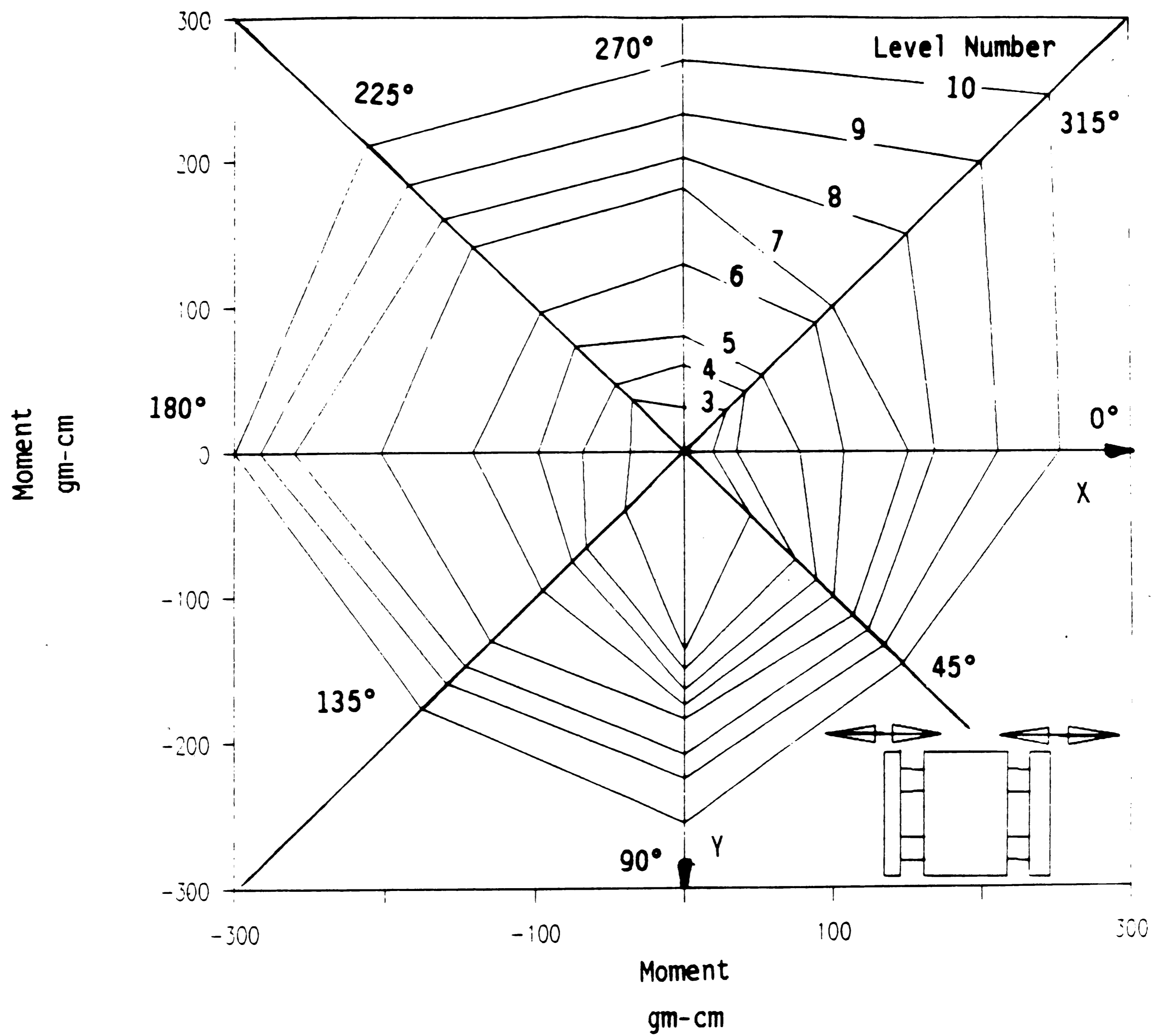
Figure 20. Adjusted Moment Data
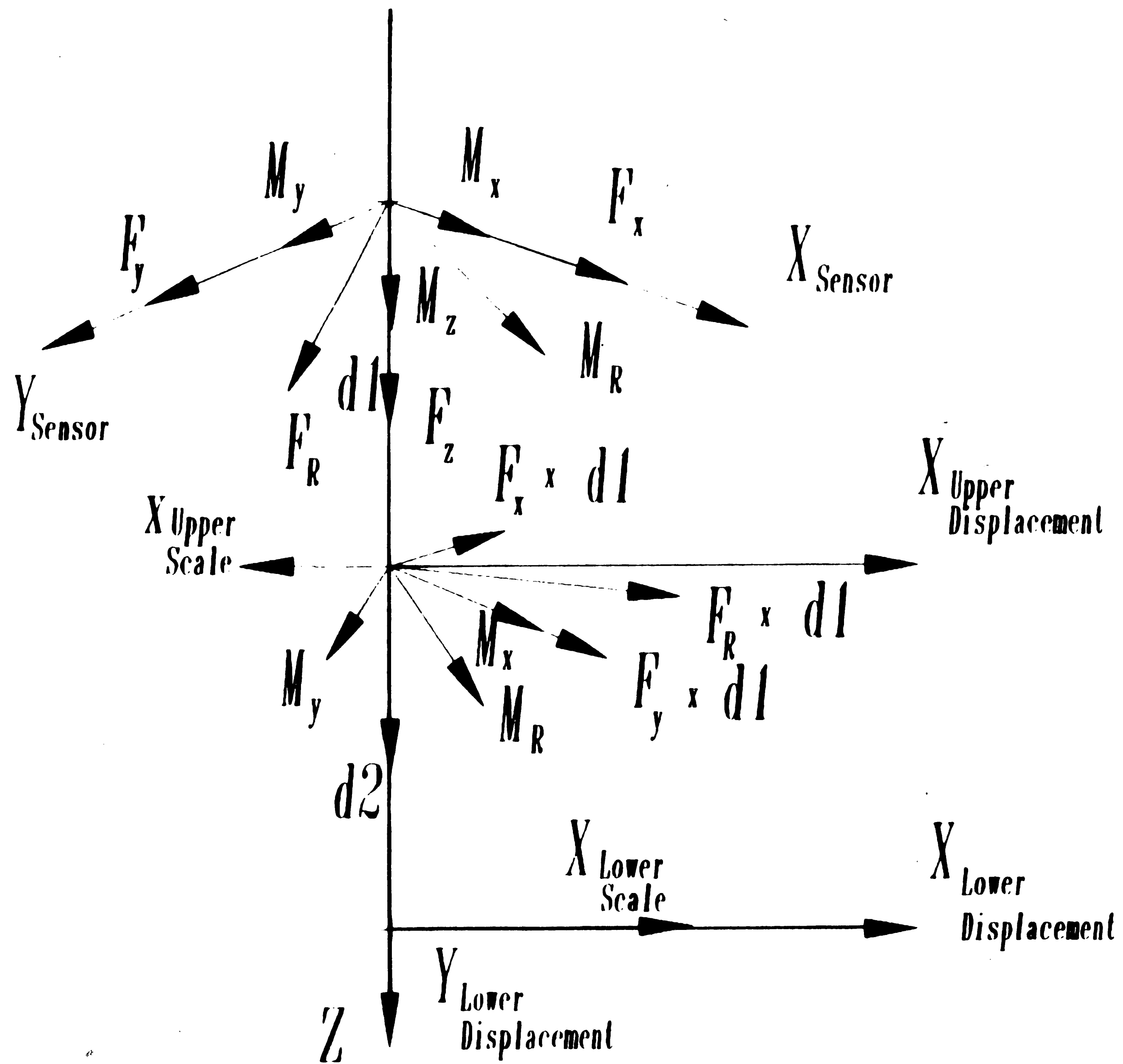
Figure 21. Schematic of Coordinate Transformation
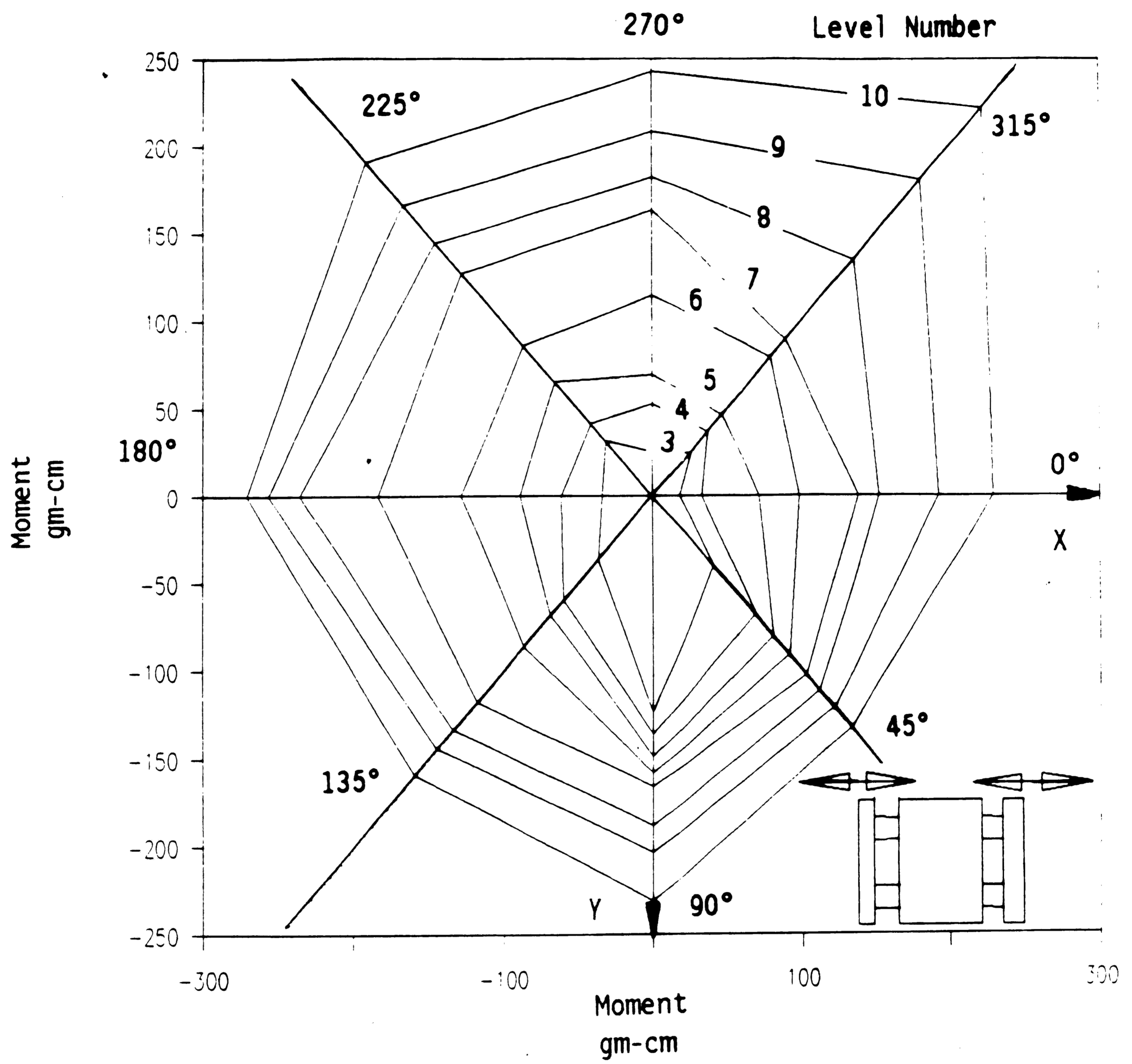
Figure 22. Total Moment
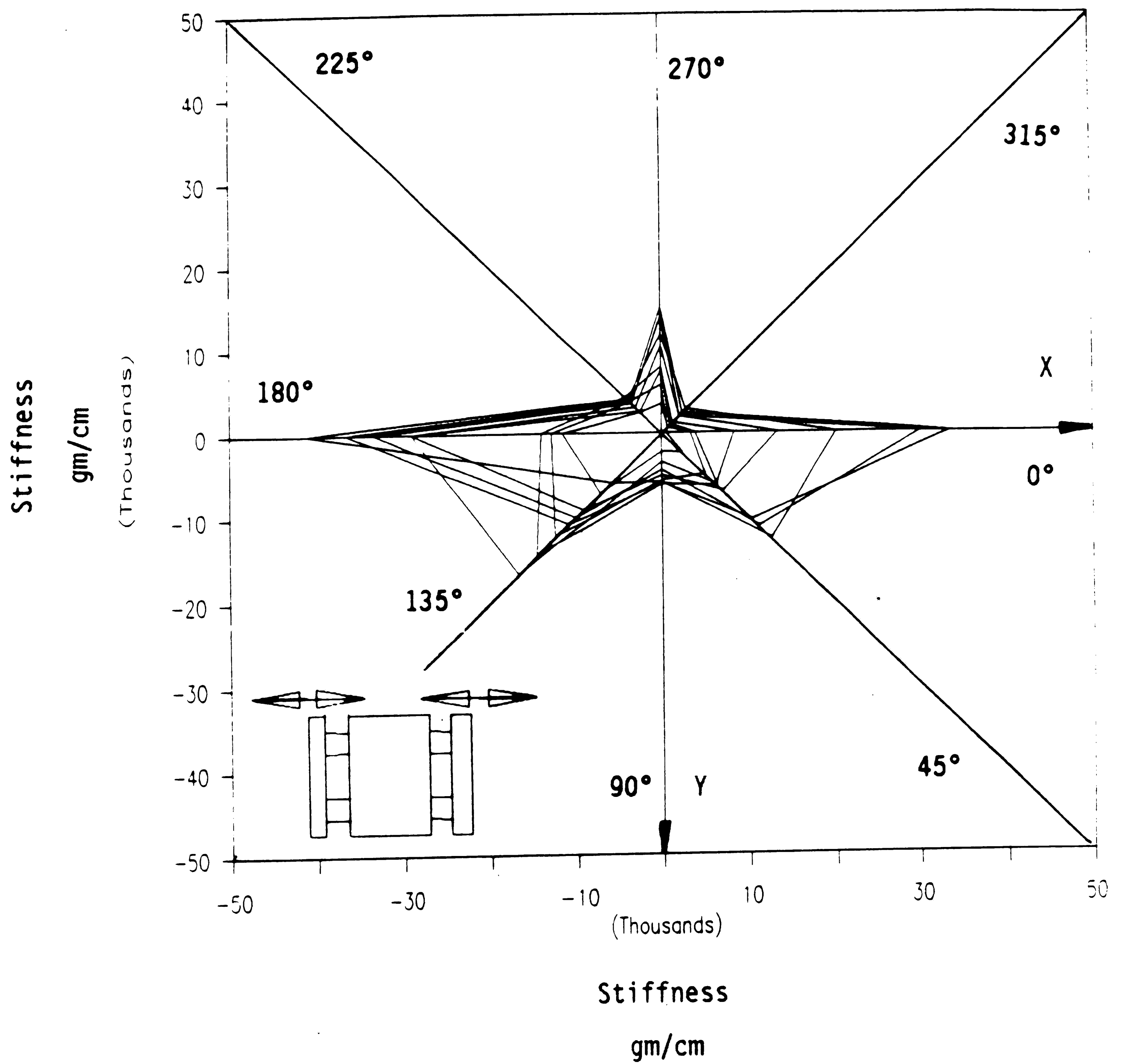
Figure 23. Unrotated Linear Stiffness
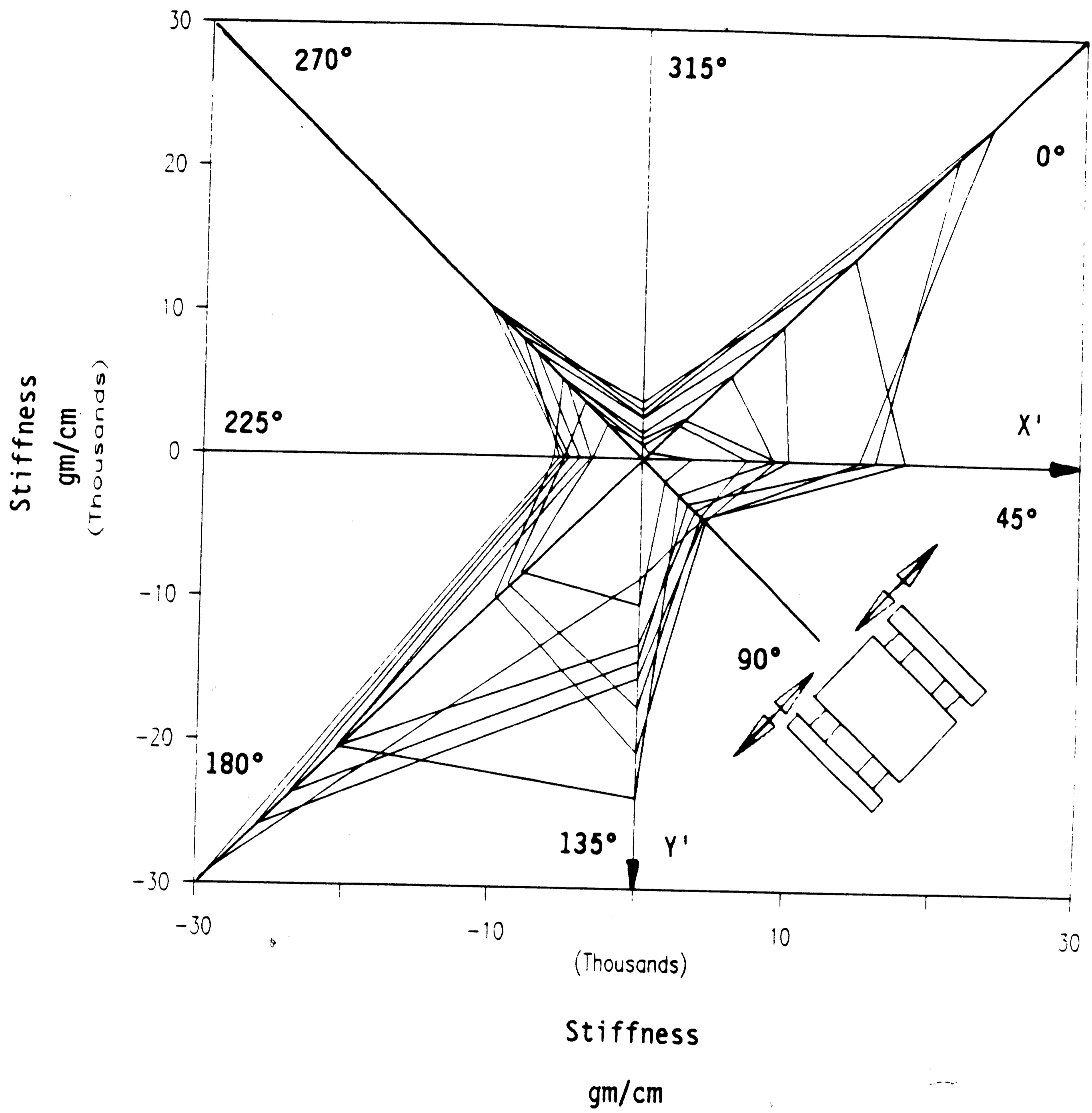
Figure 24. Rotated Linear Stiffness

44

Stiffness curves generated by a mathematical model based on an orthogonal pair of springs is superposed on that of the measured rotational stiffness contours in Fig. 27. The resulting circular and elliptic contours are such that their area is equal to that of the measured stiffness. In the case of the circle the two axial stiffnesses are equal. For the ellipse, the axial stiffnesses are chosen so that the signed sum of the shaded areas in the figure equals zero. The stiffnesses obtained using the elliptical contour are roughly the same as those from the circle. Thus an equal stiffness model is used in the following discussion.

The average rotational compliance of the system is plotted against the average angular displacement in Fig. 28. This profile indicates an increasing system stiffness as pin deflection increases.

The stiffness in Fig. 28 when substituted into the compliant insertion model given by Eq. (22), can be used to determine the displacement, δH, of the tip of the pin. This deflection increases the effective hole radius and when substituted into Eq. (23) produces the effective size ratio.

An Example

The following example is based on the experimental stiffness data. The value for K_α is obtained in a manner similar to that of K_R given above. From the experiments K_R equals 130,437 g-cm/radian, K_α equals 7,759 g/cm and K_B is determined to be equal to 9,136 g/cm.

The force (F_α), and moment (M_c), are determined from the actual forces and torques measured by the sensor. For this example F_α equals 6.3 grams while M_c equals 124 g-cm. The correction factor δH from Eq. (22):

$$\delta H = \left[\frac{6.3}{7,759} \right]$$

$$- \left[6,825 \quad \frac{124}{130,437} \right]$$

$$+ \left[\frac{6.3}{9,136}\left(1 - \frac{124^2}{130,437^2}\right) - \left[\left(\frac{6.3}{9,136}\right)\left(\frac{124}{130,437}\right)\left(1 - \frac{124^2}{130,437^2}\right)\right] \right]^{1/2} \quad (24)$$
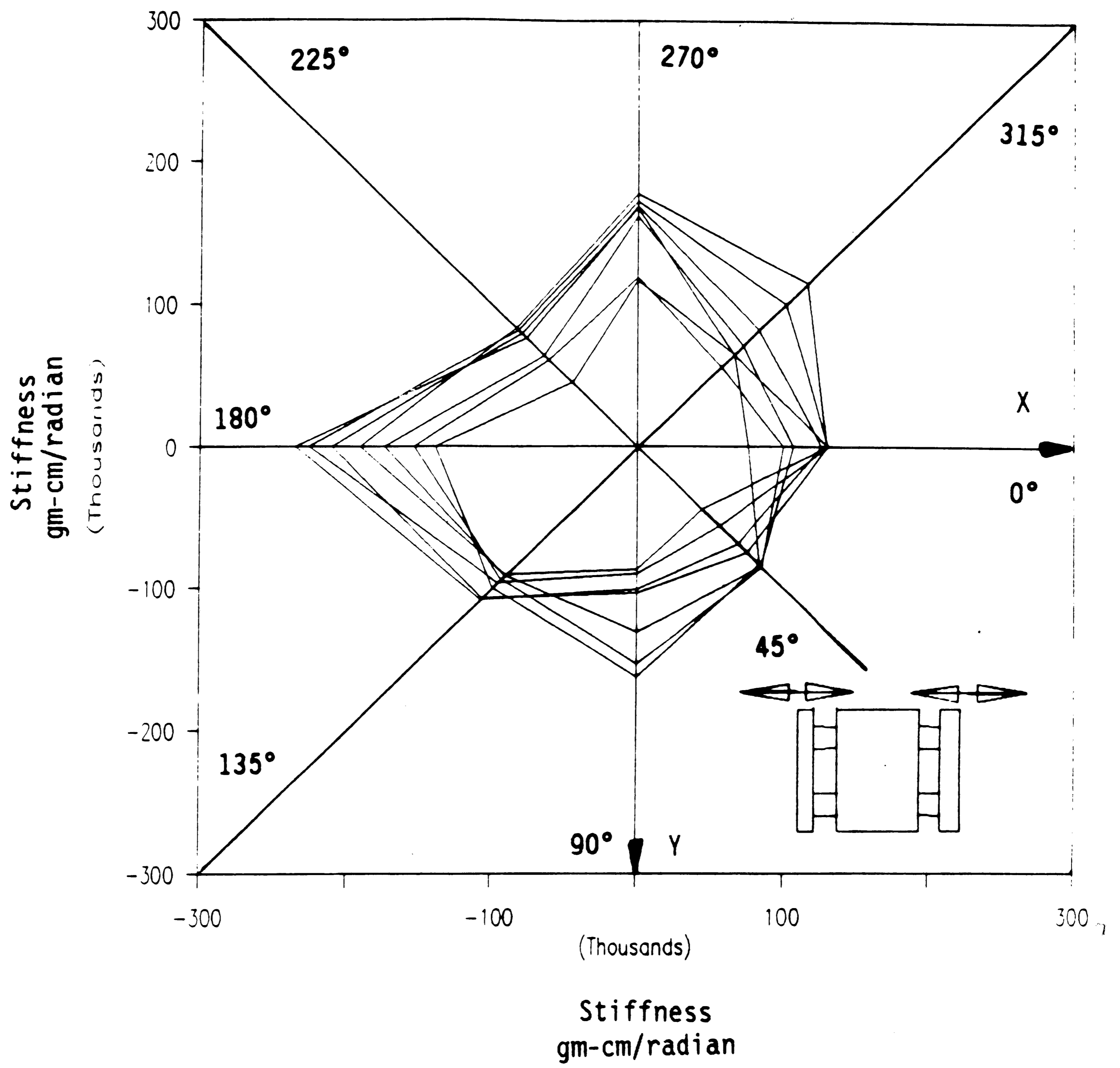
Figure 25. Unrotated Angular Stiffness
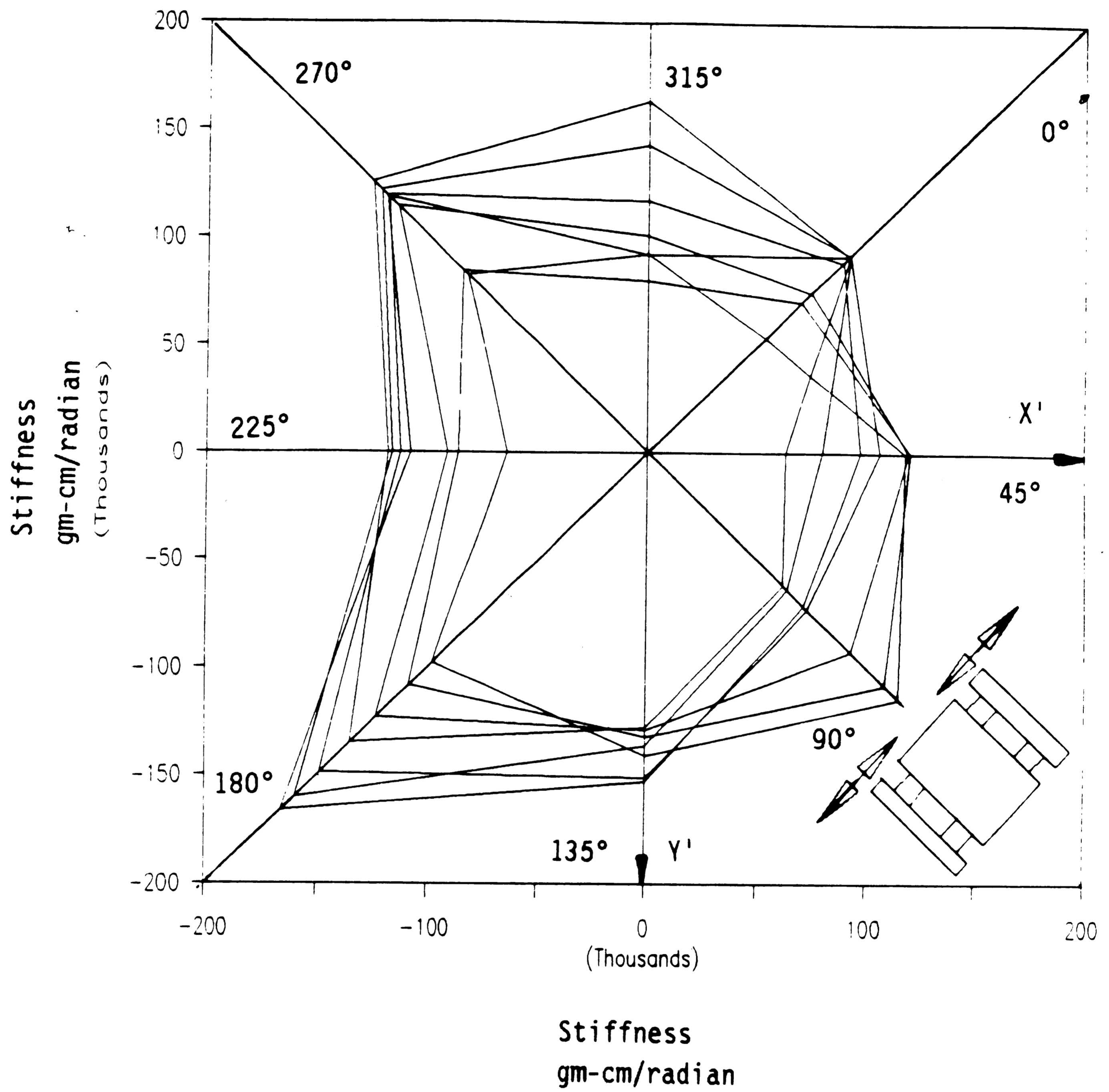
Figure 26. Rotated Angular Stiffness
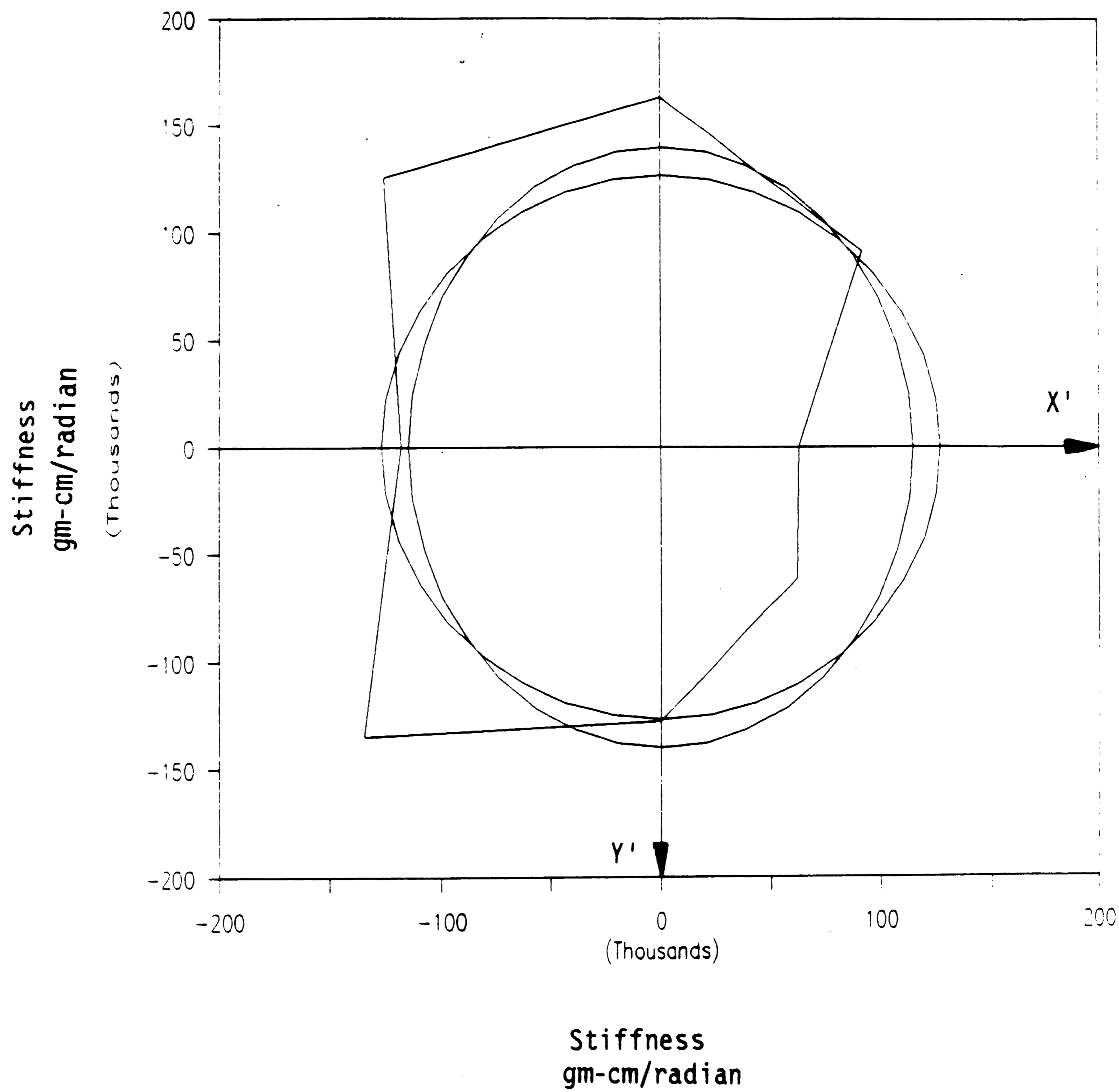
Figure 27. Equivalent Area from Actual, Elliptical
and Circular Results

48
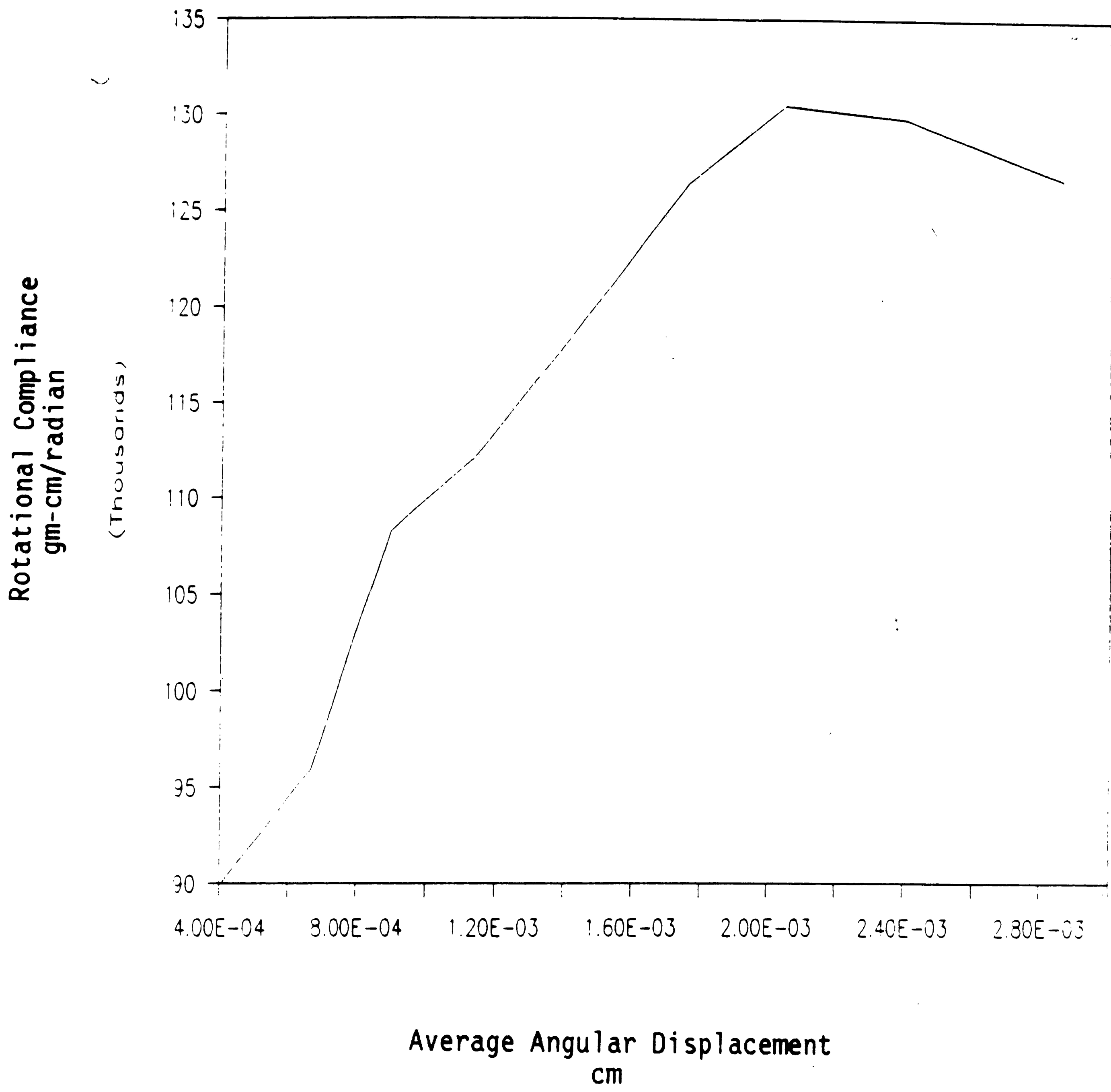
Figure 28. Rotational Compliance vs Average Angular Displacement

The y-axis is labeled "Rotational Compliance gm-cm/radian (Thousands)" with values 90, 95, 100, 105, 110, 115, 120, 125, 130, 135.

The x-axis is labeled "Average Angular Displacement cm" with values 4.00E-04, 8.00E-04, 1.20E-03, 1.60E-03, 2.00E-03, 2.40E-03, 2.30E-03.

The first of the three terms on the right hand side Eq. (24) is due to the planar stiffness, the second is due to the rotational compliance while the third is through bending. Only the second is significant. An actual size ratio of .939 results from using an actual pin size of .077 and an actual hole size of .082. Substituting the above values from the actual size ratio results in an effective size ratio of .839. Substitution of the effective size ratio into Eq. (23) results in a theoretical PSA of .265. Experimental PSA results of .225 are obtained for the actual size ratio of .939.

CHAPTER 4

RESULTS AND CONCLUSIONS

The proposed method determines the PSA from a given ratio of a peg to a hole. The model includes the affect of compliances by using an effective size ratio. The result is a tool that ensures compatibility of product design with the manufacturing process. Given three of the four parameters; tolerances, clearances, equipment precision and insertion success, the method predicts an estimate for the other.

Forces and torques were monitored for 2100 insertion attempts. In all of the 920 attempts where the insertion was successful the moments were less than 300 g-cm. In the 1180 cases which failed two types of force/torque profiles were observed. In one type of profile the axial force becomes very large and the torques remain small. We believe this indicates a stubbing failure. In the second type of profile a large axial force is supplemented by a torque greater than 300 g-cm. The torque is a result of an angular error between the pin and hole being so large that it overcame the system compliance.

An approximate value of the maximum allowable torque which occurs during successful insertions using the above system is computed based on the proposed theory. For the actual pin and hole sizes given in TABLE 1 actual size ratios are determined. An effective size ratio which would lead to the same PSA as in the experiment is then determined. The effective size ratio is then used to determine the dimensionless hole size correction, $\delta H/dP$. The angle produced by the resulting change in effective hole size is shown as alpha, α. To produce this displacement the force/torque sensor would have to experience the torque shown. This torque lays at the boundary between the insertions that failed and those that succeeded.

TABLE 1
Computed Torques
Based on Effective Size Ratio and Compliance Model

Actual Pin Size	Actual Hole Size	Actual Size Ratio	Eff. Size Ratio	del H/dP	del H	Alpha degrees	Torque
0.055	0.093	0.591	0.540	0.161	0.009	0.189	417.227
0.055	0.089	0.618	0.566	0.149	0.008	0.175	386.325
0.070	0.110	0.636	0.584	0.142	0.010	0.212	468.103
0.063	0.096	0.656	0.603	0.135	0.008	0.181	399.650
0.055	0.082	0.671	0.617	0.129	0.007	0.152	335.779
0.070	0.101	0.693	0.639	0.123	0.009	0.183	404.710
0.063	0.089	0.708	0.653	0.118	0.007	0.159	351.369
0.055	0.076	0.724	0.669	0.114	0.006	0.134	295.491
0.055	0.073	0.753	0.697	0.107	0.006	0.125	276.791
0.063	0.082	0.768	0.711	0.103	0.007	0.139	306.862
0.070	0.089	0.787	0.730	0.099	0.007	0.148	327.485
0.063	0.078	0.808	0.750	0.095	0.006	0.128	282.261
0.063	0.076	0.829	0.770	0.091	0.006	0.122	270.666
0.070	0.082	0.854	0.795	0.087	0.006	0.130	286.549
0.077	0.089	0.865	0.806	0.085	0.007	0.140	308.734
0.055	0.063	0.873	0.813	0.084	0.005	0.098	217.265
0.070	0.078	0.897	0.837	0.080	0.006	0.120	264.688
0.086	0.093	0.925	0.864	0.076	0.007	0.140	309.544
0.077	0.082	0.939	0.878	0.075	0.006	0.122	270.579
0.086	0.089	0.966	0.904	0.071	0.006	0.131	288.876
					avg.	0.146	323.448
					max.	0.212	468.103

52

REFERENCES

[1] Stoll, Henry, W., "Design for Manufacture," *Manufacturing Engineering*, January 1988..

[2] Waterbury, R., "Designing Parts for Automated Assembly," *Assembly Engineering*, February, 1985.

[3] Wick, Charles, "Designing Parts for Automated Assembly," *Manufacturing Engineering*, July 1980.

[4] Nevins, J. L.,Whitney, D. E., "Research on Advanced Assembly Automation," The Institute of Electrical and Electronics Engineers, Inc., 1977.

[5] Laktianov, N. M., Andreev, G. Y.,"The Automatic Assembly of Parts," *Russian Engineering Journal*, Vol.XLVI, No.8,1966.

[6] Kim, S., Knott, K., "The Effects of Geometric Tolerances When Assembling a Peg Into a Hole Using a Robot," Boston, The American Society of Mechanical Engineers, 1987.

[7] American National Standards Institute Y14.5M, New York, N. Y., American Society of Mechanical Engineers, 1973.

[8] Doydum, Cemal, Perreira, N. D., "A Method for Selecting Dimensions, Tolerances and Precisions for Alignment," Submitted August 1989 for Publication to The American Society of Mechanical Engineers, *Journal of Mechanisms, Transmissions, And Automation in Design*, also in ATLSS Report 89-13, NSF Engineering Research Center for Advanced Technology for Large Structural Systems, Lehigh University, Bethlehem, Pennsylvania, August 1989.

[9] Abdel-Malek, Layek, and Boucher, Thomas O.,"A Framework for the Economic Evaluation of Production System and Product Design Alternatives for Robotic Assembly," *International Journal of Production Research*, Vol.23, No.1, 1985.

[10] Abdel-Malek, Layek,"A Framework for the Robotic Assembly of Parts with General Geometries," *International Journal of Production Research*, Vol.24, No.5, 1986.

[11] Lozano-Perez, T., et al., "Automated Synthesis of Fine-Motion Strategies for Robots," *The International Journal of Robotics Research*, Vol.1, No.1, Spring 1984.

[12] Simunovic, "Force Information in the Assembly Process," The Charles Stark Draper Laboratory, Inc.

[13] Miller, I., Freund, J. E., *Probability and Statistics for Engineers*, Englewood Cliffs, New Jersey, Prentice-Hall, Inc., 1965.

[14] Holman, J. P., *Experimental Methods for Engineers*, New York, McGraw-Hill Book Company, 1989.

[15] Whitney, D. E., et al., "Designing Chamfers," *The International Journal of Robotics Research*, Vol.2, No.4, Winter 1983.

[16] Lord Corporation, "Installation and Operations Manual," USA, Lord Corporation, 1985.

ARPENDIX

TABLE 2

Force shift angle	Moment shift angle	App angle of fingers rel to lin meas	Fingers are 45 degrees to force x axis	Dir of meas force rel to force senser x axis	Exact angle Degrees	Reading
ERR	-360	0		-45	-360	1
-270	-386.5650	45		-116.5650	-341.5650	1
45	-360	90		-135	-270	1
-225	-296.5650	135		-116.5650	-161.5650	1
-206.5650	-135	180		0	45	1
180	-71.56505	225		18.434948	153.43494	1
-120.9637	-26.56505	270		18.434948	243.43494	1
ERR	-90	315		-90	225	1
ERR	0	360		-45	360	1
-360	-357.8789	0		-42.87890	-357.8789	2
-350.5376	-352.9906	45		-82.99061	-307.9906	2
18.434948	-363.9909	90		-138.9909	-273.9909	2
26.565051	-351.8698	135		-171.8698	-216.8698	2
71.565051	1.3971810	180		136.39718	181.39718	2
180	-12.09475	225		77.905242	212.90524	2
-90	-14.03624	270		30.963756	255.96375	2
0	-12.52880	315		-12.52880	302.47119	2
0	2.1210963	360		-42.87890	362.12109	2
-364.3987	-363.9004	0		-48.90049	-363.9004	3
-345.9637	-349.0193	45		-79.01934	-304.0193	3
4.3987053	-360.7073	90		-135.7073	-270.7073	3
9.4623222	-356.9059	135		-176.9059	-221.9059	3
23.198590	1.5911402	180		136.59114	181.59114	3
0	-7.594643	225		82.405356	217.40535	3
-45	-3.012787	270		41.987212	266.98721	3
0	-6.009005	315		-6.009005	308.99099	3
-4.398705	-3.900493	360		-48.90049	356.09950	3
-365.1944	-363.4566	0		-48.45661	-363.4566	4
-344.7448	-347.2635	45		-77.26359	-302.2635	4
5.7105931	-361.7357	90		-136.7357	-271.7357	4
5.7105931	-2.526116	135		177.47388	132.47388	4
15.255118	4.3044689	180		139.30446	184.30446	4

55

0	-0.954841	225	89.045158	224.04515	4
-26.56505	-4.184916	270	40.815083	265.81508	4
-11.30993	-3.270487	315	-3.270487	311.72951	4
-5.194428	-3.456619	360	-48.45661	356.54338	4
-364.3987	-361.6180	0	-46.61809	-361.6180	5
-343.7397	-345.1137	45	-75.11373	-300.1137	5
2.4895529	-360.3794	90	-135.3794	-270.3794	5
0	-3.503531	135	176.49646	131.49646	5
8.9726266	2.3532968	180	137.35329	182.35329	5
0	-0.716159	225	89.283840	224.28384	5
-15.25511	-1.636577	270	43.363422	268.36342	5
0	-1.468800	315	-1.468800	313.53119	5
-4.398705	-1.618094	360	-46.61809	358.38190	5
-363.8140	-361.7183	0	-46.71835	-361.7183	6
-344.3577	-343.3322	45	-73.33223	-298.3322	6
2.1210963	-359.7000	90	-134.7000	-269.7000	6
0	-6.072456	135	173.92754	128.92754	6
9.4623222	2.0771747	180	137.07717	182.07717	6
0	-0.440728	225	89.559271	224.55927	6
-10.30484	-1.618094	270	43.381905	268.38190	6
0	1.0708244	315	1.0708244	316.07082	6
-3.814074	-1.718358	360	-46.71835	358.28164	6
-361.7357	-361.0139	0	-46.01397	-361.0139	7
-344.3577	-344.5259	45	-74.52598	-299.5259	7
0	-361.7623	90	-136.7623	-271.7623	7
-2.045408	-6.527841	135	173.47215	128.47215	7
4.3987053	0.4034847	180	135.40348	180.40348	7
-2.385944	0	225	90	225	7
-6.842773	-2.862405	270	42.137594	267.13759	7
-2.489552	-1.145762	315	-1.145762	313.85423	7
-1.735704	-1.013978	360	-46.01397	358.98602	7
-363.1798	-360	0	-45	-360	8
-344.5778	-343.2215	45	-73.22154	-298.2215	8
-2.602562	-363.7102	90	-138.7102	-273.7102	8
-6.170175	-9.752424	135	170.24757	125.24757	8
2.6025622	-0.355869	180	134.64413	179.64413	8
-2.121096	-0.564472	225	89.435527	224.43552	8
-5.710593	-0.763898	270	44.236101	269.23610	8
-2.385944	-0.341042	315	-0.341042	314.65895	8
-3.179830	0	360	-45	360	8
-361.4688	-359.3562	0	-44.35625	-359.3562	9
-340.4633	-340.7581	45	-70.75812	-295.7581	9
-1.218875	-363.0697	90	-138.0697	-273.0697	9
-5.710593	-9.362387	135	170.63761	125.63761	9

1.1233027	-0.465809	180	134.53419	179.53419	9
-1.909152	-0.737673	225	89.262326	224.26232	9
-2.045408	0.8593722	270	45.859372	270.85937	9
-1.789910	-0.543071	315	-0.543071	314.45692	9
-1.468800	0.6437457	360	-44.35625	360.64374	9
-361.3322	-359.2151	0	-44.21517	-359.2151	10
-341.0753	-340.7841	45	-70.78411	-295.7841	10
-4.573921	-365.8726	90	-140.8726	-275.8726	10
-5.440332	-9.996899	135	170.00310	125.00310	10
1.9091524	-0.135450	180	134.86454	179.86454	10
-6.340191	-4.447384	225	85.552615	220.55261	10
-1.684684	0.3486515	270	45.348651	270.34865	10
0	0.6820603	315	0.6820603	315.68206	10
-1.332219	0.7848246	360	-44.21517	360.78482	10

Force/Torque Output

Fx	Fy			Fz	Mx	My
0	0	ERR	ERR	-1	0	0
0	-1	-1	-1.08E-19	0	-1	-2
-1	0	-0.707106	0.7071067	0	0	0
-1	-1	-2.71E-19	1.4142135	0	-1	-2
-3	-1	2.2360679	2.2360679	3	1	0
-2	0	2	0	4	3	1
-4	-1	2.9154759	-2.915475	6	3	1
0	0	ERR	ERR	0	0	-2
0	0	ERR	ERR	-1	0	0
-2	-2	-2	-2	1	14	-13
-18	-3	-18.24828	2.596E-15	1	15	-122
-4	2	-3.162277	3.1622776	0	-23	-20
-2	4	5.204E-17	4.4721359	-1	-28	-4
-1	2	1.5811388	1.5811388	3	-21	20
-1	0	1	0	4	3	14
-2	-2	2	-2	6	15	9
0	-2	0	-2	0	9	-2
-2	-2	-2	-2	1	14	-13
-7	-6	-6.519202	-6.519202	2	41	-47
-20	-5	-20.61552	-8.90E-15	-3	26	-134
-7	6	-6.519202	6.5192024	-1	-41	-40
-1	6	-8.05E-17	6.0827625	0	-37	-2
2	5	3.8078865	3.8078865	2	-37	35
1	0	1	0	5	4	30
0	-3	2.1213203	-2.121320	6	30	27
0	-2	0	-2	0	19	-2
-7	-6	-6.519202	-6.519202	2	41	-47
-12	-10	-11.04536	-11.04536	2	70	-79
-22	-6	-22.80350	1.084E-14	-4	33	-146
-11	9	-10.04987	10.049875	-2	-68	-64
-1	10	-6.42E-17	10.049875	-1	-68	3
4	7	5.7008771	5.7008771	2	-50	43
6	0	6	0	2	1	60
2	-6	4.4721359	-4.472135	6	44	38
-1	-5	8.186E-18	-5.099019	0	35	-2
-12	-10	-11.04536	-11.04536	2	70	-79
-14	-12	-13.03840	-13.03840	1	86	-91
-24	-7	-25	1.158E-15	-4	42	-158
-12	11	-11.51086	11.510864	1	-76	-75

58

0	14	0	14	-2	-98	6
8	11	9.6176920	9.6176920	3	-76	70
7	0	7	0	4	1	80
4	-7	5.7008771	-5.700877	4	54	51
0	-11	0	-11	-1	78	-2
-14	-12	-13.03840	-13.03840	1	86	-91
-16	-14	-15.03329	-15.03329	2	97	-103
-25	-7	-25.96150	1.544E-16	-2	50	-167
-14	13	-13.50925	13.509256	0	-95	-96
0	20	0	20	-3	-141	15
10	14	12.165525	12.165525	3	-100	93
15	0	15	0	0	1	130
9	-13	11.180339	-11.18033	2	91	86
0	-16	0	-16	-1	107	2
-16	-14	-15.03329	-15.03329	2	97	-103
-17	-16	-16.50757	-16.50757	0	111	-115
-25	-7	-25.96150	1.544E-16	-4	49	-177
-19	19	-19	19	2	-134	-126
1	28	-4.82E-17	28.017851	-7	-201	23
18	21	19.557607	19.557607	1	-143	141
24	-1	24.020824	-1.45E-17	-1	0	182
11	-14	12.589678	-12.58967	2	105	95
-1	-23	1.924E-17	-23.02172	-3	150	-3
-17	-16	-16.50757	-16.50757	0	111	-115
-19	-17	-18.02775	-18.02775	-1	123	-123
-29	-8	-30.08321	9.032E-15	-2	60	-199
-21	23	-22.02271	22.022715	1	-156	-137
4	37	1.765E-16	37.215588	-9	-256	44
21	23	22.022715	22.022715	0	-160	162
27	-1	27.018512	-5.02E-17	-2	2	203
18	-22	20.099751	-20.09975	-1	152	148
-1	-24	-1.45E-17	-24.02082	-4	168	-1
-19	-17	-18.02775	-18.02775	-1	123	-123
-20	-19	-19.50640	-19.50640	-1	135	-132
-31	-11	-32.89376	-3.71E-15	-2	74	-212
-23	24	-23.50531	23.505318	2	-167	-150
4	40	2.567E-16	40.199502	-9	-279	46
25	26	25.504901	25.504901	-2	-183	186
30	-1	30.016662	2.884E-17	-4	3	233
27	-29	28.017851	-28.01785	-3	197	203
-1	-32	5.258E-17	-32.01562	-4	211	-2
-20	-19	-19.50640	-19.50640	-1	135	-132
-22	-21	-21.50581	-21.50581	2	148	-144
-35	-12	-37	1.048E-14	-3	84	-241

-23	27	-25.07987	25.079872	-2	-193	-157
4	42	-8.93E-17	42.190046	-9	-295	52
29	31	30.016662	30.016662	-3	-211	212
36	-4	36.221540	2.229E-16	6	21	270
33	-35	34.014702	-34.01470	-8	245	248
0	-37	0	-37	-6	252	3
-22	-21	-21.50581	-21.50581	2	148	-144

		Mz	Actual Fxl g	Actual Fyl g	Moment Due To Fy Mx g-cm	Moment Due To Fx My g-cm	Measured Moment Mx g-cm
0	0	-1	ERR	ERR	ERR	ERR	0
-5.28E-16	-2.236067	-1	-0.2	-2.17E-20	7.921E-20	-0.7306	-4.22E-16
0	0	0	-0.141421	0.1414213	-0.516612	-0.516612	0
-2.236067	-1.69E-15	-1	-5.42E-20	0.2828427	-1.033224	-1.98E-19	-1.788854
-0.707106	0.7071067	-1	0.4472135	0.4472135	-1.633671	1.6336712	-0.565685
7.474E-16	3.1622776	-1	0.4	0	0	1.4612	5.979E-16
2.2360679	2.2360679	-2	0.5830951	-0.583095	2.1300467	2.1300467	1.7888543
2	0	-1	ERR	ERR	ERR	ERR	!.6
0	0	-1	ERR	ERR	ERR	ERR	0
13.509256	-13.50925	-2	-0.4	-0.4	1.4612	-1.4612	10.807404
6.733E-14	-122.9186	0	-3.649657	5.193E-16	-1.90E-15	-13.33219	5.386E-14
-21.55226	-21.55226	-1	-0.632455	0.6324555	-2.310360	-2.310360	-17.24180
-28.28427	-1.34E-14	-2	1.041E-17	0.8944271	-3.267342	3.802E-17	-22.62741
-20.50609	20.506096	0	0.3162277	0.3162277	-1.155180	1.1551800	-16.40487
-8.55E-16	14.317821	-2	0.2	0	0	0.7306	-6.84E-16
12.369316	12.369316	-3	0.4	-0.4	1.4612	1.4612	9.8954535
9.2195444	1.803E-15	-1	0	-0.4	1.4612	0	7.3756355
13.509256	-13.50925	-2	-0.4	-0.4	1.4612	-1.4612	10.807404
44.102154	-44.10215	-3	-1.303840	-1.303840	4.7629292	-4.762929	35.281723
5.588E-14	-136.4990	-2	-4.123105	-1.78E-15	6.504E-15	-15.06170	4.471E-14
-40.50308	-40.50308	-2	-1.303840	1.3038404	-4.762929	-4.762929	-32.40246
-37.05401	-1.70E-14	-2	-1.61E-17	1.2165525	-4.444066	-5.88E-17	-29.64321
-36.01388	36.013886	-1	0.7615773	0.7615773	-2.782041	2.7820419	-28.81110
-1.86E-15	30.265491	-1	0.2	0	0	0.7306	-1.49E-15
28.539446	28.539446	-5	0.4242640	-0.424264	1.5498366	1.5498366	22.831557
19.104973	4.034E-15	-1	0	-0.4	1.4612	0	15.283978
44.102154	-44.10215	-3	-1.303840	-1.303840	4.7629292	-4.762929	35.281723
74.635782	-74.63578	-3	-2.209072	-2.209072	8.0697407	-8.069740	59.708625
8.319E-14	-149.6829	-3	-4.560701	2.168E-15	-7.92E-15	-16.66024	6.656E-14
-66.03029	-66.03029	-3	-2.009975	2.0099751	-7.342439	-7.342439	-52.82423
-68.06614	-1.45E-14	-3	-1.28E-17	2.0099751	-7.342439	-4.69E-17	-54.45291
-46.63153	46.631534	-2	1.1401754	1.1401754	-4.165060	4.1650608	-37.30522
-4.21E-16	60.008332	-1	1.2	0	0	4.3836	-3.37E-16
41.109609	41.109609	-4	0.8944271	-0.894427	3.2673425	3.2673425	32.887687
35.057096	5.442E-16	-2	1.637E-18	-1.019803	3.7253436	5.980E-18	28.045677
74.635782	-74.63578	-3	-2.209072	-2.209072	8.0697407	-8.069740	59.708625
88.535303	-88.53530	-4	-2.607680	-2.607680	9.5258585	-9.525858	70.828242
5.409E-14	-163.4870	-3	-5	2.317E-16	-8.46E-16	-18.265	4.327E-14
-75.50165	-75.50165	-3	-2.302172	2.3021728	-8.409837	-8.409837	-60.40132

-98.18350	-2.71E-15	-4	0	2.8	-10.2284	0	-78.54680
-73.06161	73.061617	-1	1.9235384	1.9235384	-7.026685	7.0266857	-58.44929
1.930E-14	80.006249	-1	1.4	0	0	5.1142	1.544E-14
52.521424	52.521424	-3	1.1401754	-1.140175	4.1650608	4.1650608	42.017139
78.025636	3.455E-14	-2	0	-2.2	8.0366	0	62.420509
88.535303	-88.53530	-4	-2.607680	-2.607680	9.5258585	-9.525858	70.828242
100.04498	-100.0449	-5	-3.006659	-3.006659	10.983326	-10.98332	80.035991
8.433E-14	-174.3244	-4	-5.192301	3.088E-17	-1.13E-16	-18.96747	6.747E-14
-95.50130	-95.50130	-3	-2.701851	2.7018512	-9.869862	-9.869862	-76.40104
-141.7956	-2.47E-14	2	0	4	-14.612	0	-113.4365
-96.56345	96.563450	-1	2.4331050	2.4331050	-8.888132	8.8881326	-77.25076
2.227E-14	130.00384	-2	3	0	0	10.959	1.782E-14
88.535303	88.535303	-4	2.2360679	-2.236067	8.1683563	8.1683563	70.828242
107.01868	-4.37E-14	-2	0	-3.2	11.6896	0	85.614951
100.04498	-100.0449	-5	-3.006659	-3.006659	10.983326	-10.98332	80.035991
113.01769	-113.0176	-5	-3.301514	-3.301514	12.060433	-12.06043	90.414158
3.220E-14	-183.6572	-4	-5.192301	3.088E-17	-1.13E-16	-18.96747	2.576E-14
-130.0615	-130.0615	-4	-3.8	3.8	-13.8814	-13.8814	-104.0492
-202.3116	6.720E-15	3	-9.65E-18	5.6035702	-20.46984	-3.52E-17	-161.8493
-142.0035	142.00352	-2	3.9115214	3.9115214	-14.28878	14.288787	-113.6028
0	182	-2	4.8041648	-2.89E-18	1.057E-17	17.549614	0
100.12492	100.12492	-4	2.5179356	-2.517935	9.1980189	9.1980189	80.099937
150.02999	7.117E-14	-2	3.849E-18	-4.604345	16.819675	1.406E-17	120.02399
113.01769	-113.0176	-5	-3.301514	-3.301514	12.060433	-12.06043	90.414158
123	-123	-6	-3.605551	-3.605551	13.171078	-13.17107	98.4
9.305E-15	-207.8485	-4	-6.016643	1.806E-15	-6.60E-15	-21.97879	7.444E-15
-146.8076	-146.8076	-3	-4.404543	4.4045431	-16.08979	-16.08979	-117.4461
-259.7537	5.292E-14	5	3.530E-17	7.4431176	-27.18970	1.290E-16	-207.8029
-161.0031	161.00310	0	4.4045431	4.4045431	-16.08979	16.089795	-128.8024
6.115E-14	203.00985	-2	5.4037024	-1.00E-17	3.668E-17	19.739724	4.892E-14
150.01333	150.01333	-5	4.0199502	-4.019950	14.684878	14.684878	120.01066
168.00297	7.560E-14	-3	-2.89E-18	-4.804164	17.549614	-1.06E-17	134.40238
123	-123	-6	-3.605551	-3.605551	13.171078	-13.17107	98.4
133.50842	-133.5084	-6	-3.901281	-3.901281	14.251382	-14.25138	106.80674
-9.03E-15	-224.5439	-4	-6.578753	-7.41E-16	2.708E-15	-24.03218	-7.23E-15
-158.7277	-158.7277	-4	-4.701063	4.7010637	-17.17298	-17.17298	-126.9822
-282.7666	3.911E-14	4	5.135E-17	8.0399004	-29.36975	1.876E-16	-226.2133
-184.5060	184.50609	1	5.1009802	5.1009802	-18.63388	18.633881	-147.6048
6.356E-14	233.01931	-2	6.0033324	5.768E-18	-2.11E-17	21.930173	5.085E-14
200.02249	200.02249	-6	5.6035702	-5.603570	20.469842	20.469842	160.01799
211.00947	8.647E-15	-3	1.052E-17	-6.403124	23.390612	3.842E-17	168.80758
133.50842	-133.5084	-6	-3.901281	-3.901281	14.251382	-14.25138	106.80674
146.01369	-146.0136	-6	-4.301162	-4.301162	15.712147	-15.71214	116.81095
3.089E-14	-255.2195	-6	-7.4	2.096E-15	-7.66E-15	-27.0322	2.471E-14

-175.9232	-175.9232	-4	-5.015974	5.0159744	-18.32335	-18.32335	-140.7386
-299.5479	-2.57E-14	4	-1.79E-17	8.4380092	-30.82404	-6.53E-17	-239.6383
-211.5005	211.50059	1	6.0033324	6.0033324	-21.93017	21.930173	-169.2004
1.564E-14	270.81543	-2	7.2443081	4.458E-17	-1.63E-16	26.463457	1.251E-14
246.50456	246.50456	-6	6.8029405	-6.802940	24.851141	24.851141	197.20365
252.01785	-4.58E-14	-3	0	-7.4	27.0322	0	201.61428
146.01369	-146.0136	-6	-4.301162	-4.301162	15.712147	-15.71214	116.81095
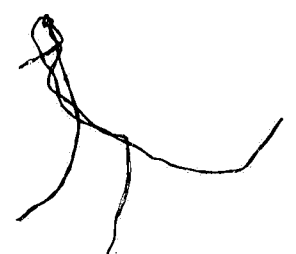
Transformed Values

Measured Moment My g-cm	Total Xl Moment Mx g-cm	Total Yl Moment My g-cm	Lower Scale	Lower disp in	Upper disp in	About ym Rot Disp rad	Along xm Lin Disp cm
0	ERR	ERR	7.406	0	0	0	0
-1.788854	-4.22E-16	-2.519454	7.402	0	0	0	0
0	-0.516612	-0.516612	7.418	0	0	0	0
-1.35E-15	-2.822078	-1.35E-15	7.433	0	0	0	0
0.5656854	-2.199356	2.1993566	7.447	0	0	0	0
2.5298221	5.979E-16	3.9910221	7.457	0	0	0	0
1.7888543	3.9189011	3.9189011	7.446	0	0	0	0
0	ERR	ERR	7.43	0	0	0	0
0	ERR	ERR	7.406	0	0	0	0
-10.80740	12.268604	-12.26860	7.408	0.002	0	0.0007443	0
-98.33493	5.196E-14	-111.6671	7.4035	0.0015	-0.0002	0.0006326	-0.000508
-17.24180	-19.55216	-19.55216	7.419	0.001	-0.0002	0.0004465	-0.000508
-1.07E-14	-25.89475	-1.07E-14	7.4335	0.0005	-0.0002	0.0002605	-0.000508
16.404877	-17.56005	17.560057	7.448	0.001	-0.0001	0.0004093	-0.000254
11.454256	-6.84E-16	12.184856	7.4575	0.0005	-0.0001	0.0002232	-0.000254
9.8954535	11.356653	11.356653	7.447	0.001	0	0.0003721	0
1.443E-15	8.8368355	1.443E-15	7.4305	0.0005	0	0.0001860	0
-10.80740	12.268604	-12.26860	7.408	0.002	0	0.0007443	0
-35.28172	40.044652	-40.04465	7.4085	0.0025	-0.0001	0.0009676	-0.000254
-109.1992	5.121E-14	-124.2609	7.404	0.002	-0.0002	0.0008187	-0.000508
-32.40246	-37.16539	-37.16539	7.4195	0.0015	-0.0003	0.0006698	-0.000762
-1.36E-14	-34.08727	-1.36E-14	7.434	0.001	-0.0002	0.0004465	-0.000508
28.811108	-31.59315	31.593150	7.449	0.002	-0.0006	0.0009676	-0.001524
24.212393	-1.49E-15	24.942993	7.458	0.001	-0.0002	0.0004465	-0.000508
22.831557	24.381393	24.381393	7.4475	0.0015	-0.0001	0.0005954	-0.000254
3.227E-15	16.745178	3.227E-15	7.431	0.001	-0.0001	0.0004093	-0.000254
-35.28172	40.044652	-40.04465	7.4085	0.0025	-0.0001	0.0009676	-0.000254
-59.70862	67.778366	-67.77836	7.409	0.003	-0.0001	0.0011537	-0.000254
-119.7463	5.864E-14	-136.4066	7.405	0.003	-0.0002	0.0011909	-0.000508
-52.82423	-60.16667	-60.16667	7.42	0.002	-0.0003	0.0008559	-0.000762
-1.16E-14	-61.79535	-1.17E-14	7.4345	0.0015	-0.0002	0.0006326	-0.000508
37.305227	-41.47028	41.470288	7.4495	0.0025	-0.001	0.0013025	-0.00254
48.006666	-3.37E-16	52.390266	7.4585	0.0015	-0.0002	0.0006326	-0.000508
32.887687	36.155030	36.155030	7.448	0.002	-0.0001	0.0007815	-0.000254
4.353E-16	31.771020	4.413E-16	7.4315	0.0015	-0.0001	0.0005954	-0.000254
-59.70862	67.778366	-67.77836	7.409	0.003	-0.0001	0.0011537	-0.000254
-70.82824	80.354101	-80.35410	7.4095	0.0035	-0.0001	0.0013397	-0.000254
-130.7896	4.243E-14	-149.0546	7.4055	0.0035	-0.0002	0.0013770	-0.000508
-60.40132	-68.81116	-68.81116	7.4205	0.0025	-0.0003	0.0010420	-0.000762

-2.17E-15	-88.77520	-2.17E-15	7.435	0.002	-0.0002	0.0008187	-0.000508
58.449294	-65.47598	65.475980	7.45	0.003	-0.0011	0.0015258	-0.002794
64.004999	1.544E-14	69.119199	7.459	0.002	-0.0002	0.0008187	-0.000508
42.017139	46.182200	46.182200	7.449	0.003	-0.0001	0.0011537	-0.000254
2.764E-14	70.457109	2.764E-14	7.4325	0.0025	-0.0002	0.0010048	-0.000508
-70.82824	80.354101	-80.35410	7.4095	0.0035	-0.0001	0.0013397	-0.000254
-80.03599	91.019318	-91.01931	7.41	0.004	-0.0001	0.0015258	-0.000254
-139.4595	6.735E-14	-158.4270	7.4065	0.0045	-0.0001	0.0017119	-0.000254
-76.40104	-86.27090	-86.27090	7.421	0.003	-0.0006	0.0013397	-0.001524
-1.98E-14	-128.0485	-1.98E-14	7.4355	0.0025	-0.0003	0.0010420	-0.000762
77.250760	-86.13889	86.138893	7.451	0.004	-0.0011	0.0018980	-0.002794
104.00307	1.782E-14	114.96207	7.4595	0.0025	-0.0002	0.0010048	-0.000508
70.828242	78.996599	78.996599	7.45	0.004	-0.0002	0.0015630	-0.000508
-3.50E-14	97.304551	-3.50E-14	7.433	0.003	-0.0005	0.0013025	-0.00127
80.03599	91.019318	-91.01931	7.41	0.004	-0.0001	0.0015258	-0.000254
-90.41415	102.47459	-102.4745	7.411	0.005	-0.0002	0.0019352	-0.000508
-146.9258	2.565E-14	-165.8933	7.408	0.006	-0.0001	0.0022701	-0.000254
-104.0492	-117.9306	-117.9306	7.4215	0.0035	-0.0007	0.0015630	-0.001778
5.376E-15	-182.3191	5.341E-15	7.436	0.003	-0.0003	0.0012281	-0.000762
113.60281	-127.8916	127.89160	7.452	0.005	-0.0011	0.0022701	-0.002794
145.6	1.057E-17	163.14961	7.4605	0.0035	-0.0002	0.0013770	-0.000508
80.099937	89.297956	89.297956	7.451	0.005	-0.0002	0.0019352	-0.000508
5.694E-14	136.84367	5.695E-14	7.4335	0.0035	-0.0005	0.0014886	-0.00127
-90.41415	102.47459	-102.4745	7.411	0.005	-0.0002	0.0019352	-0.000508
-98.4	111.57107	-111.5710	7.412	0.006	-0.0002	0.0023074	-0.000508
-166.2788	8.451E-16	-188.2576	7.409	0.007	-0.0001	0.0026423	-0.000254
-117.4461	-133.5359	-133.5359	7.422	0.004	-0.0007	0.0017491	-0.001778
4.233E-14	-234.9926	4.246E-14	7.4365	0.0035	-0.0003	0.0014142	-0.000762
128.80248	-144.8922	144.89228	7.453	0.006	-0.0012	0.0026795	-0.003048
162.40788	4.896E-14	182.14760	7.461	0.004	-0.0001	0.0015258	-0.000254
120.01066	134.69554	134.69554	7.452	0.006	-0.0002	0.0023074	-0.000508
6.048E-14	151.95199	6.047E-14	7.434	0.004	-0.0006	0.0017119	-0.001524
-98.4	111.57107	-111.5710	7.412	0.006	-0.0002	0.0023074	-0.000508
-106.8067	121.05812	-121.0581	7.414	0.008	-0.0002	0.0030517	-0.000508
-179.6351	-4.52E-15	-203.6673	7.4105	0.0085	-0.0001	0.0032005	-0.000254
-126.9822	-144.1551	-144.1551	7.423	0.005	-0.0007	0.0021213	-0.001778
3.129E-14	-255.5831	3.148E-14	7.437	0.004	-0.0003	0.0016002	-0.000762
147.60487	-166.2387	166.23875	7.4535	0.0065	-0.0012	0.0028656	-0.003048
186.41545	5.083E-14	208.34562	7.4615	0.0045	-0.0001	0.0017119	-0.000254
160.01799	180.48784	180.48784	7.4525	0.0065	-0.0003	0.0025307	-0.000762
6.917E-15	192.19819	6.956E-15	7.435	0.005	-0.0006	0.0020841	-0.001524
-106.8067	121.05812	-121.0581	7.414	0.008	-0.0002	0.0030517	-0.000508
-116.8109	132.52310	-132.5231	7.417	0.011	-0.0004	0.0042426	-0.001016
-204.1756	1.705E-14	-231.2078	7.412	0.01	-0.0001	0.0037588	-0.000254

-140.7386	-159.0619	-159.0619	7.424	0.006	-0.0007	0.0024934	-0.001778
-2.05E-14	-270.4624	-2.06E-14	7.438	0.005	-0.0004	0.0020096	-0.001016
169.20047	-191.1306	191.13064	7.4545	0.0075	-0.0012	0.0032378	-0.003048
216.65234	1.235E-14	243.11580	7.462	0.005	-0.0002	0.0019352	-0.000508
197.20365	222.05479	222.05479	7.453	0.007	-0.0003	0.0027167	-0.000762
-3.66E-14	228.64648	-3.66E-14	7.436	0.006	-0.0007	0.0024934	-0.001778
-116.8109	132.52310	-132.5231	7.417	0.011	-0.0004	0.0042426	-0.001016

xm in +fxl direct	xm in +fyl direct	y rot disp in +fxl direct	in +fyl direct
0	0	0	0
0	0	0	0
0	0	0	0
0	0	0	0
0	0	0	0
0	0	0	0
0	0	0	0
0	0	0	0
0	0	0	0
0	0	0.0005263	0.0005263
-0.000359	0.0003592	0.0004473	0.0004473
-0.000359	0.0003592	0.0003157	0.0003157
-0.000359	0.0003592	0.0001842	0.0001842
-0.000179	0.0001796	0.0002894	0.0002894
-0.000179	0.0001796	0.0001578	0.0001578
0	0	0.0002631	0.0002631
0	0	0.0001315	0.0001315
0	0	0.0005263	0.0005263
-0.000179	0.0001796	0.0006842	0.0006842
-0.000359	0.0003592	0.0005789	0.0005789
-0.000538	0.0005388	0.0004736	0.0004736
-0.000359	0.0003592	0.0003157	0.0003157
-0.001077	0.0010776	0.0006842	0.0006842
-0.000359	0.0003592	0.0003157	0.0003157
-0.000179	0.0001796	0.0004210	0.0004210
-0.000179	0.0001796	0.0002894	0.0002894
-0.000179	0.0001796	0.0006842	0.0006842
-0.000179	0.0001796	0.0008157	0.0008157
-0.000359	0.0003592	0.0008421	0.0008421
-0.000538	0.0005388	0.0006052	0.0006052
-0.000359	0.0003592	0.0004473	0.0004473
-0.001796	0.0017960	0.0009210	0.0009210
-0.000359	0.0003592	0.0004473	0.0004473
-0.000179	0.0001796	0.0005526	0.0005526
-0.000179	0.0001796	0.0004210	0.0004210
-0.000179	0.0001796	0.0008157	0.0008157
-0.000179	0.0001796	0.0009473	0.0009473
-0.000359	0.0003592	0.0009736	0.0009736
-0.000538	0.0005388	0.0007368	0.0007368

```
-0.000359  0.0003592  0.0005789  0.0005789
-0.001975  0.0019756  0.0010789  0.0010789
-0.000359  0.0003592  0.0005789  0.0005789
-0.000179  0.0001796  0.0008157  0.0008157
-0.000359  0.0003592  0.0007105  0.0007105
-0.000179  0.0001796  0.0009473  0.0009473
-0.000179  0.0001796  0.0010789  0.0010789
-0.000179  0.0001796  0.0012105  0.0012105
-0.001077  0.0010776  0.0009473  0.0009473
-0.000538  0.0005388  0.0007368  0.0007368
-0.001975  0.0019756  0.0013421  0.0013421
-0.000359  0.0003592  0.0007105  0.0007105
-0.000359  0.0003592  0.0011052  0.0011052
-0.000898  0.0008980  0.0009210  0.0009210
-0.000179  0.0001796  0.0010789  0.0010789
-0.000359  0.0003592  0.0013684  0.0013684
-0.000179  0.0001796  0.0016052  0.0016052
-0.001257  0.0012572  0.0011052  0.0011052
-0.000538  0.0005388  0.0008684  0.0008684
-0.001975  0.0019756  0.0016052  0.0016052
-0.000359  0.0003592  0.0009736  0.0009736
-0.000359  0.0003592  0.0013684  0.0013684
-0.000898  0.0008980  0.0010526  0.0010526
-0.000359  0.0003592  0.0013684  0.0013684
-0.000359  0.0003592  0.0016315  0.0016315
-0.000179  0.0001796  0.0018684  0.0018684
-0.001257  0.0012572  0.0012368  0.0012368
-0.000538  0.0005388  0.0010000  0.0010000
-0.002155  0.0021552  0.0018947  0.0018947
-0.000179  0.0001796  0.0010789  0.0010789
-0.000359  0.0003592  0.0016315  0.0016315
-0.001077  0.0010776  0.0012105  0.0012105
-0.000359  0.0003592  0.0016315  0.0016315
-0.000359  0.0003592  0.0021578  0.0021578
-0.000179  0.0001796  0.0022631  0.0022631
-0.001257  0.0012572  0.0015000  0.0015000
-0.000538  0.0005388  0.0011315  0.0011315
-0.002155  0.0021552  0.0020263  0.0020263
-0.000179  0.0001796  0.0012105  0.0012105
-0.000538  0.0005388  0.0017894  0.0017894
-0.001077  0.0010776  0.0014736  0.0014736
-0.000359  0.0003592  0.0021578  0.0021578
-0.000718  0.0007184  0.0030000  0.0030000
-0.000179  0.0001796  0.0026579  0.0026579
```

```
-0.001257  0.0012572  0.0017631  0.0017631
-0.000718  0.0007184  0.0014210  0.0014210
-0.002155  0.0021552  0.0022894  0.0022894
-0.000359  0.0003592  0.0013684  0.0013684
-0.000538  0.0005388  0.0019210  0.0019210
-0.001257  0.0012572  0.0017631  0.0017631
-0.000718  0.0007184  0.0030000  0.0030000
```

DISPLACEMENT		ROTATIONAL		ROTATED		
kx	ky	kx	ky	kx	ky	
ERR	ERR	ERR	ERR	ERR	ERR	0
ERR	ERR	ERR	ERR	ERR	ERR	45
ERR	ERR	ERR	ERR	ERR	ERR	90
ERR	ERR	ERR	ERR	ERR	ERR	135
ERR	ERR	ERR	ERR	ERR	ERR	180
ERR	ERR	ERR	ERR	ERR	ERR	225
ERR	ERR	ERR	ERR	ERR	ERR	270
ERR	ERR	ERR	ERR	ERR	ERR	315
ERR	ERR	ERR	ERR	ERR	ERR	360
ERR	ERR	23310.299	-23310.29	32965.741	-7.72E-12	0
10160.226	1.446E-12	1.162E-10	-249608.3	176499.76	-176499.7	45
1760.6834	1760.6834	-61915.07	-61915.07	5.659E-11	-87561.13	90
-2.90E-14	2489.9824	-140571.2	-5.79E-11	-99398.88	-99398.88	135
-1760.683	1760.6834	-60661.88	60661.886	-85788.86	-1.03E-11	180
-1113.553	0	-4.33E-12	77170.594	-54567.85	54567.850	225
ERR	ERR	43155.190	43155.190	0	61030.655	270
ERR	ERR	67159.806	1.096E-11	47489.154	47489.154	315
ERR	ERR	23310.299	-23310.29	32965.741	-7.72E-12	360
7259.4838	-7259.483	58526.674	-58526.67	82769.216	2.573E-11	0
11478.251	-4.96E-12	8.846E-11	-214632.1	151767.83	-151767.8	45
2419.8279	2419.8279	-78460.11	-78460.11	6.174E-11	-110959.3	90
4.482E-14	3386.7422	-107942.8	-4.32E-11	-76327.09	-76327.09	135
-706.7145	706.71454	-46174.50	46174.506	-65300.61	-1.03E-11	180
-556.7769	0	-4.71E-12	78985.976	-55851.51	55851.519	225
-2362.204	-2362.204	57905.685	57905.685	5.148E-12	81891.006	270
0	-2227.107	57846.856	1.115E-11	40903.904	40903.904	315
7259.4838	-7259.483	58526.674	-58526.67	82769.216	2.573E-11	360
12299.605	-12299.60	83082.980	-83082.98	117497.07	1.029E-11	0
12696.468	6.035E-12	6.963E-11	-161982.5	114538.95	-114538.9	45
3730.3596	3730.3596	-99405.59	-99405.59	2.058E-11	-140580.7	90
3.574E-14	5595.5395	-138130.4	-2.61E-11	-97673.01	-97673.01	135
-634.8234	634.82344	-45024.78	45024.787	-63674.66	5.146E-12	180
-3340.661	0	-7.53E-13	117107.40	-82807.43	82807.438	225
-4979.964	-4979.964	65423.247	65423.247	-2.57E-11	92522.443	270
-9.12E-15	-5678.033	75456.012	1.048E-12	53355.457	53355.457	315
12299.605	-12299.60	83082.980	-83082.98	117497.07	1.029E-11	360
14518.967	-14518.96	84818.036	-84818.03	119950.81	2.058E-11	0
13919.424	6.449E-13	4.357E-11	-153082.7	108245.86	-108245.8	45
4272.6563	4272.6563	-93386.37	-93386.37	-2.06E-11	-132068.2	90

0	7794.8779	-153338.6	-3.74E-12	-108426.8	-108426.8	135
-973.6199	973.61993	-60684.92	60684.924	-85821.44	5.144E-12	180
-3897.438	0	2.667E-11	119387.45	-84419.67	84419.677	225
-6348.234	-6348.234	56610.317	56610.317	1.029E-11	80059.078	270
0	-6124.546	99161.644	3.890E-11	70117.871	70117.871	315
14518.967	-14518.96	84818.036	-84818.03	119950.81	2.058E-11	360
16740.387	-16740.38	84359.187	-84359.18	119301.90	3.087E-11	0
28909.542	1.719E-13	5.564E-11	-130874.2	92542.036	-92542.03	45
2507.2143	2507.2143	-91063.54	-91063.54	2.058E-11	-128783.2	90
0	7423.6932	-173779.7	-2.68E-11	-122880.8	-122880.8	135
-1231.542	1231.5426	-64181.78	64181.782	-90766.74	1.543E-11	180
-8351.654	0	2.507E-11	161798.13	-114408.5	114408.55	225
-6224.956	-6224.956	71472.960	71472.960	-2.06E-11	101078.02	270
0	-3563.372	105644.71	-3.80E-11	74702.094	74702.094	315
16740.387	-16740.38	84359.187	-84359.18	119301.90	3.087E-11	360
9191.0374	-9191.037	74885.117	-74885.11	105903.54	-3.09E-11	0
28909.542	1.719E-13	1.598E-11	-103343.1	73074.643	-73074.64	45
3022.5036	3022.5036	-106698.9	-106698.9	7.203E-11	-150895.0	90
1.791E-14	10399.796	-209942.8	6.150E-12	-148451.9	-148451.9	135
-1979.859	1979.8592	-79670.00	79670.008	-112670.4	0	180
-13374.24	-8.06E-15	1.086E-14	167558.70	-118481.8	118481.89	225
-7009.643	-7009.643	65256.058	65256.058	4.116E-11	92286.003	270
-4.29E-15	-5127.187	130001.20	5.410E-11	91924.737	91924.737	315
9191.0374	-9191.037	74885.117	-74885.11	105903.54	-3.09E-11	360
10037.439	-10037.43	68382.127	-68382.12	96706.931	0	0
33499.287	1.006E-11	4.523E-13	-100757.3	71246.221	-71246.22	45
3503.3546	3503.3546	-107965.0	-107965.0	5.144E-11	-152685.5	90
-6.55E-14	13813.855	-234992.1	4.246E-11	-166164.5	-166164.5	135
-2043.623	2043.6235	-76470.76	76470.761	-108145.9	-1.03E-11	180
-30086.57	-5.59E-14	4.538E-11	168819.37	-119373.3	119373.32	225
-11191.07	-11191.07	82555.156	82555.156	5.145E-11	116750.62	270
2.686E-15	-4458.080	125525.29	4.996E-11	88759.785	88759.785	315
10037.439	-10037.43	68382.127	-68382.12	96706.931	0	360
10860.719	-10860.71	56099.985	-56099.98	79337.360	-1.03E-11	0
36628.986	-4.13E-12	-2.00E-12	-89992.36	63634.212	-63634.21	45
3739.2058	3739.2058	-96103.25	-96103.25	3.087E-11	-135910.5	90
-9.53E-14	14921.438	-225863.6	2.782E-11	-159709.7	-159709.7	135
-2366.757	2366.7570	-82039.73	82039.730	-116021.7	0	180
-33425.17	3.211E-14	4.199E-11	172111.23	-121701.0	121701.01	225
-10399.79	-10399.79	100860.63	100860.63	-4.12E-11	142638.47	270
-9.76E-15	-5941.853	130419.92	4.720E-12	92220.812	92220.812	315
10860.719	-10860.71	56099.985	-56099.98	79337.360	-1.54E-11	360
5986.9709	-5986.970	44174.273	-44174.27	62471.856	5.144E-12	0
41201.497	1.167E-11	6.415E-12	-86988.89	61510.434	-61510.43	45

3989.6845	3989.6845	-90214.06	-90214.06	-1.03E-11	-127581.9	90
2.487E-14	11745.223	-190325.0	-1.45E-11	-134580.1	-134580.1	135
-2785.431	2785.4311	-83482.17	83482.171	-118061.6	1.029E-11	180
-20167.32	1.241E-13	9.025E-12	177661.16	-125625.4	125625.41	225
-12625.73	-12625.73	115589.91	115589.91	-4.12E-11	163468.82	270
0	-5885.928	129679.81	-2.08E-11	91697.478	91697.478	315
5986.9709	-5986.970	44174.273	-44174.27	62471.856	5.144E-12	360

Area Formulation

	ERR	ERR	ERR
	ERR		
	ERR	ERR	ERR
	ERR		
	ERR	ERR	ERR
	ERR		
	ERR	ERR	ERR
	ERR		
	ERR		
3.115E+10	-7.85E+09	-1.27E+10	
1.064E+10			
9.88E+09	-5.88E+08	-6.76E+08	
8.62E+09			
2.98E+09	176330697	851831743	
4.01E+09			
2.26E+09	321537229	-3.45E+08	
2.23E+09			
2.549E+10			
2.303E+10	-3.10E+09	-5.24E+09	
1.470E+10			
5.83E+09	1.32E+09	-4.21E+08	
6.73E+09			
3.12E+09	727172449	263873101	
4.11E+09			
1.67E+09	838266248	856227362	
3.37E+09			
2.891E+10			
1.312E+10	1.49E+09	169410320	
1.478E+10			
9.54E+09	2.10E+09	-1.66E+09	
9.98E+09			
6.86E+09	402237361	-7.92E+08	
6.47E+09			
2.85E+09	1.04E+09	1.71E+09	
5.60E+09			
3.683E+10			
1.172E+10	1.29E+09	633506133	
1.364E+10			
1.176E+10	1.28E+09	-1.23E+09	
1.181E+10			
7.13E+09	-1.84E+08	59168313.	

7.00E+09

4.92E+09 348528142 1.75E+09

7.01E+09

3.947E+10

8.56E+09 1.68E+09 1.24E+09

1.148E+10

1.510E+10 362649983 -1.97E+09

1.349E+10

1.309E+10 -7.63E+08 -1.35E+09

1.097E+10

5.58E+09 985168797 1.67E+09

8.23E+09

4.417E+10

5.34E+09 2.84E+09 1.20E+09

9.38E+09

2.204E+10 181337399 -2.66E+09

1.956E+10

1.404E+10 -1.55E+09 -3.44E+08

1.214E+10

8.45E+09 16604660. 642499314

9.11E+09

5.020E+10

5.08E+09 2.90E+09 906989700

8.88E+09

2.761E+10 -1.12E+09 -4.82E+09

2.167E+10

1.425E+10 -1.57E+08 -6.70E+08

1.342E+10

7.88E+09 1.24E+09 352693523

9.47E+09

5.345E+10

4.05E+09 2.30E+09 499628724

6.85E+09

2.551E+10 -1.90E+09 -3.49E+09

2.012E+10

1.481E+10 1.27E+09 -3.46E+08

1.574E+10

8.50E+09 2.32E+09 -5.94E+08

1.024E+10

5.294E+10

3.78E+09 2.03E+09 29568758.

5.85E+09

1.811E+10 -4.71E+08 -1.11E+09

1.653E+10

1.578E+10   2.38E+09 -4.75E+08
1.768E+10
 8.41E+09   3.29E+09 -1.34E+09
1.036E+10
5.042E+10

Biography

Name: Michael F. Laub

Date of Birth: March 4, 1959

Place of Birth: Columbus, Ohio

Father's Name: James S. Laub

Mother's Name: Marilyn U. Laub

Education: Lehigh University

                                             M.S.M.E., October 1989

                                             Syracuse University

                                             B.S.M.E., December 1983

Professional: Machine Design Engineer

                                             Amp, Incorporated

                                             Harrisburg, PA

                                             [6/84 - Present]

                                             Mechanical Engineer

                                             Texmark Division

                                             Syracuse, NY

                                             [5/81 - 5/84]